

Toward Millijoule-Level High-Power Ultrafast Thin-Disk Oscillators

Clara J. Saraceno, Florian Emaury, Cinia Schriber, Andreas Diebold, Martin Hoffmann, Matthias Golling, Thomas Südmeyer, and Ursula Keller, *Fellow, IEEE*

(Invited Paper)

Abstract—SESAM modelocked thin-disk lasers have recently reached new frontiers and remain the leading technology in terms of average power and pulse energy, setting new performance levels for ultrafast oscillators. The milestones achieved seem to indicate that there are no major roadblocks ahead to achieve further scaling of modelocked oscillators to kilowatt output powers and millijoule output pulse energies. In this paper, we review the current state of the art and present the next steps toward future generations of millijoule, kilowatt-class ultrafast thin-disk oscillators.

Index Terms—High-power lasers, ultrafast lasers, modelocking, semiconductor saturable absorber mirror (SESAM), thin-disk laser (TDL).

I. INTRODUCTION

ULTRAFast laser sources have enormous impact on many disciplines of science and technology. A growing number of research areas, for example in physics, chemistry, medicine and biology daily rely on laser sources that produce pulses with femtosecond to few picosecond pulse durations, and that reach peak powers sufficient to unveil phenomena that occur on this timescale. Traditional Ti:Sapphire oscillators and amplifiers still remain the main workhorse for most applications in research. However, growing needs for faster acquisition times and higher yields are currently boosting demands for ultrafast sources with ever-increasing average power, i.e. ultrafast sources that combine high peak power and high repetition rate.

One important example that has been driving the development of such sources is the field of strong-field physics [1], [2], for

Manuscript received April 14, 2014; revised June 24, 2014; accepted July 15, 2014. Date of publication July 22, 2014; date of current version September 3, 2014. This work was supported by the Swiss National Science Foundation and the authors acknowledge support from the FIRST cleanroom facility for advanced micro- and nanotechnology of ETH Zurich for the SESAM fabrication. This work was also supported by the Swiss National Science Foundation and the FIRST cleanroom facilities of ETH Zurich for the SESAM growth. The work of T. Südmeyer was supported by the ERC (ERC starting grant 2011 #279545 “Efficient megahertz XUV light source”).

C. J. Saraceno is with the Swiss Federal Institute of Technology (ETH Zurich), 8093, Zurich, Switzerland, and also with the University of Neuchâtel, 2000, Neuchâtel, Switzerland (e-mail: saraceno@phys.ethz.ch).

F. Emaury, C. Schriber, A. Diebold, M. Golling, and U. Keller are with the Swiss Federal Institute of Technology (ETH Zurich), 8093, Zurich, Switzerland (e-mail: emaur@phys.ethz.ch; cschriber@phys.ethz.ch; diebolda@phys.ethz.ch; golling@phys.ethz.ch; keller@phys.ethz.ch).

M. Hoffmann and T. Südmeyer are with the University of Neuchâtel, 2000, Neuchâtel, Switzerland (e-mail: martin.hoffmann@unine.ch; thomas.sudmeyer@unine.ch).

Color versions of one or more of the figures in this paper are available online at <http://ieeexplore.ieee.org>.

Digital Object Identifier 10.1109/JSTQE.2014.2341588

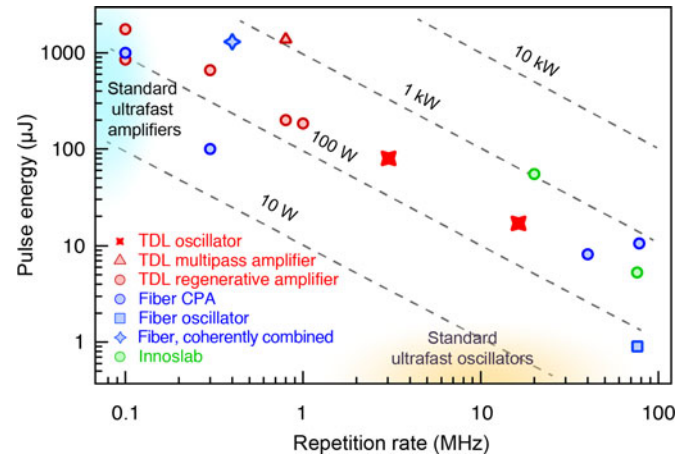


Fig. 1. Overview of state-of-the-art ultrafast sources combining high repetition rate and high pulse energy [8]–[11], [14]–[20]. The dashed lines represent constant average power. Current modelocked thin-disk oscillators with record high pulse energy and high average power (red crosses) achieve comparable performance to that of amplifier systems at megahertz repetition rates.

example high-harmonic generation (HHG) [3] or attosecond science [4]. The highly nonlinear processes involved in such experiments typically require long integration and therefore long measurement times, which is exacerbated when using systems that operate at low repetition rates (typically in the kHz regime) [1].

Another prominent application field that has also played a major role in boosting research on ultrafast high average power laser systems is in industry, for high-speed and high-precision micromachining of a wide variety of materials including metals, glasses and semiconductors [5]. The increasing speed of available scanners now justifies the use of laser systems with very high repetition rates [6]. For these applications, sources with a few picoseconds pulse durations are typically sufficient, but some specific materials benefit from femtosecond pulse durations [7].

The progress made in the last years in the field of ultrafast high-power sources has been tremendous [8]–[11]. The main drivers of this progress have been diode-pumped solid-state laser technologies, mostly based on amplifier chains. The common point between all these technologies, namely fiber, slab and disk, is the outstanding cooling geometry of the gain medium, which is suitable for high average power operation and power scaling (see Fig. 1). Among these laser geometries, the thin disk concept

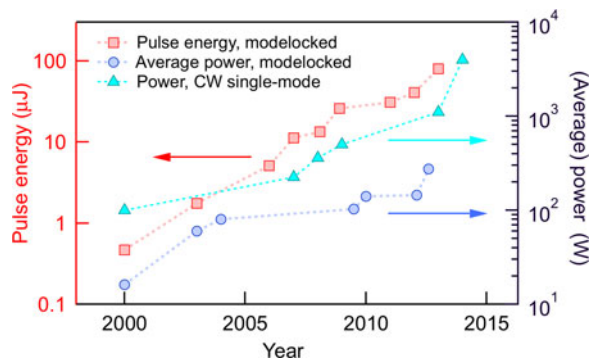


Fig. 2. Evolution of average power and pulse energy from modelocked thin disk lasers since their first demonstration in the year 2000, together with the evolution of the maximum power in single-transverse fundamental mode CW operation from a single-disk resonator.

[12], [13] is ideally suited for short pulses as both nonlinearities and thermal distortions are kept to a minimum.

The use of thin disk technology for power scaling of ultrafast sources, both modelocked oscillators and amplifiers, has gained significant ground in the past few years [9], [11], [17], [18]. High-power modelocked thin-disk lasers (TDLs) are an elegant option among these power-scalable technologies. Unprecedented high energy and average power levels can be reached directly from a passively modelocked oscillator without any extra amplification. This has many potential advantages compared to amplifier systems with similar performance: for example in terms of noise level and pulse quality, but also in terms of reliability, long-term stability and complexity provided that the required industrial engineering effort is applied to these systems, which remain to-date only available in research environments. Since their first demonstration in the year 2000 [21], modelocked TDLs have outperformed other types of ultrafast oscillators in terms of output average power and pulse energy and a steady increase in the achievable levels illustrates the potential for further scaling (see Fig. 2).

Most of the energy and power scaling of modelocked TDLs has been achieved with Yb:YAG as gain material [22]. This material has outstanding properties for TDLs and benefits from many years of industrial development, making disks with outstanding quality commercially available. In terms of average power, 275 W have been achieved with an Yb:YAG TDL operated in a vacuum chamber to reduce the parasitic nonlinearity caused by the air inside the oscillator. The repetition rate of this TDL was 16.3 MHz and the obtained pulse duration was 583 fs, resulting in a pulse energy of 17 μJ and a peak power of 26 MW [11]. Using the same concept to reduce nonlinearity, energy scaling was successfully achieved and resulted in the recent demonstration of a pulse energy of 80 μJ . In this case, the oscillator operated at a repetition rate of 3 MHz and an average power of 242 W [18]. The pulse duration achieved was 1.07 ps, and the resulting peak power of the sech^2 -shaped pulses was 66 MW.

Although Yb:YAG is the most commonly used gain material for power and energy scaling in the thin disk geometry, it is worth noting that a large number of other suitable Yb-doped materials

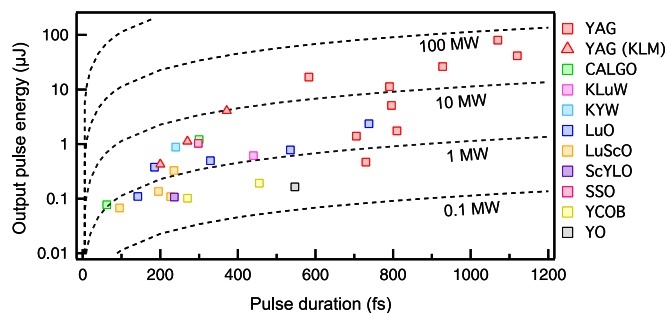


Fig. 3. Output pulse energy versus pulse duration of modelocked TDLs demonstrated to date, illustrating the current ongoing challenge of reducing the pulse duration available with $>10 \mu\text{J}$ to the sub-100 fs regime. The dashed curves represent constant peak power. An overview of the different results presented in this graph is given in [30].

are currently being investigated. In particular, an important area of research is devoted to extending the record performance of TDLs to the short pulse duration regime (<200 fs), using appropriate gain materials with broad gain bandwidths [23]–[27].

In Fig. 3, the output pulse energy versus pulse duration of modelocked TDLs demonstrated to-date based on different Yb-doped materials is illustrated. As we can see, TDLs with pulse durations <200 fs remain limited in output pulse energy, and current systems with high pulse energies still require challenging external pulse compression schemes to reach this performance [28], [29]. The difficulties involved in the generation of high-energy levels, which will be discussed in this paper, are greatly increased for shorter pulse durations as nonlinearities scale with intracavity peak power. In addition, the quality of the available broadband materials is not yet comparable with that of Yb:YAG. However, it is expected that the quality of these novel materials as well as the corresponding contacting techniques will keep improving, which will support the goal of combining record-high average power and pulse energy levels with these extremely short pulse durations. In the meantime, this remains one of the crucial milestones not yet achieved for such lasers.

One important group of materials that are outstanding candidates in this goal are Yb-doped cubic sesquioxides [31], [32]. Their potential for the thin-disk geometry has already been confirmed. In 2010, a modelocked TDL based on Yb:Lu₂O₃ with 141 W of average power at a pulse duration of 738 fs was demonstrated [33], which held the record for the highest average power from a modelocked TDL for many years. With this same material, pulses as short as 142 fs were achieved at moderate average power (7 W) [34], but indicating the potential for power scaling with very short pulse durations. In 2012, using the mixed sesquioxide crystal Yb:LuScO₃ the sub-100 fs milestone was reached for the first time [35], followed in 2013 by the demonstration of an Yb:CALGO TDL reaching 62 fs [36], which currently holds the record of the shortest pulses obtained to-date from a modelocked TDL. Although the power levels in these initial proof-of-principle sub-100 fs demonstrations are limited to the sub-10 W regime, we can expect power scaling to several tens of microjoules and hundreds of watts, similar to what is currently achieved with Yb:YAG, in the near future.

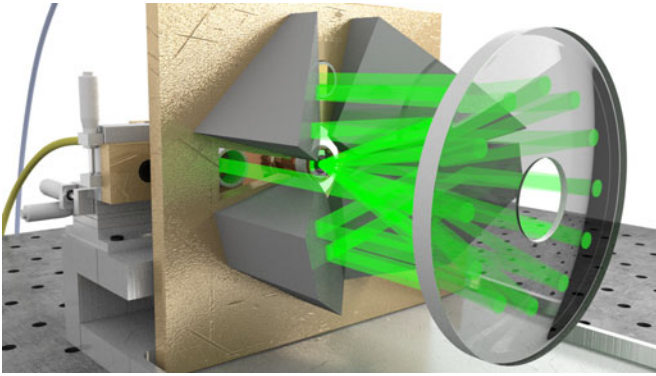


Fig. 4. Schematic view of the pumping scheme of TDLs, illustrating a 24-pump pass pumping module.

In this paper, we discuss the next steps toward the future generation of kW-class modelocked oscillators with pulse energies in the millijoule range. Recent results show that single fundamental transverse mode TDLs can reach up to 4 kW of continuous-wave (CW) power (see Fig. 2) [37], which should support kW-level modelocked oscillators with the targeted high pulse energies. We will review recent progress, current limitations and discuss alternatives to overcome them. We will focus on harnessing nonlinearities and thermal effects on different intracavity components, and address SESAM optimization for the targeted levels, aiming for minimizing oscillator complexity. The currently reached milestones allow us to foresee that millijoule-level, kilowatt-class oscillators appear feasible in the near future.

II. MODELLOCKING OF HIGH-POWER THIN DISK LASERS

A. Power Scaling Considerations

The excellent cooling scheme of the disk geometry [12], [13] allows for straightforward power scaling with minimal thermal lensing and aberrations and therefore for operation with a fundamental Gaussian beam even at very high output power. Stable single transverse mode operation is a crucial requirement for passive modelocking and a Gaussian beam results in the highest peak power for a given pulse energy. Power scalability of TDLs is based on the use of a very thin gain medium (typically $<200 \mu\text{m}$) contacted (typically glued or soldered) on a water-cooled heatsink. Until recently, most commonly used heatsinks were copper alloys (copper or copper-tungsten) with a thermal expansion coefficient matched to that of the disk. However, the use of disks glued on diamond [38] has proved to yield best performance in recent results both in CW [37], [39] and pulsed operation [9], [11], [17]. The gain disk has a highly reflective coating on the backside and an anti-reflective coating on the front side for both the pump and laser wavelengths and can therefore be used in reflection in a laser resonator (see Fig. 5). Efficient pumping of the disk-shaped gain medium is achieved by recycling the unabsorbed single-pass pump light in a multi-pass geometry (see Fig. 4). Typical commercially available thin-disk pumping modules are arranged for 24

pump passes through the thin disk (but modules exist with up to 44 passes).

If the thickness of the disk is negligible compared to the pump spot diameter (typically more than one order of magnitude), the heat flow is nearly one-dimensional. In this configuration, increasing the spot size area and power by the same factor will keep intensity, thermal gradients and maximum temperature constant on the disk. For applications where beam quality is not of primary importance, this concept can be applied nearly without restrictions: these limits are discussed in detail in [13]. The highest CW power demonstrated so far from one single disk in a multimode resonator is 6 kW [37], which is still far from the limits suggested in [13]. However, for passive modelocking, stable single-transverse mode operation is crucial. Different transverse modes have slightly different sets of longitudinal modes, and instabilities occur when trying to simultaneously lock these modes in phase. The fundamental Gaussian mode provides the highest peak intensity, and is therefore favorable. It is therefore not surprising that progress achieved in the average power of modelocked TDLs goes hand-in-hand with progress achieved in power scaling of TDLs in single fundamental transverse-mode in CW operation (see Fig. 2). In this case, the requirements on the contacting, gain material quality and resonator design are significantly more stringent. Residual small thermal aberrations need to be compensated by an appropriate cavity design [40], [41] or with adaptive optics [42]. Very recently, an impressive 4 kW of CW power was reported with a measured M^2 of 1.38, using Yb:YAG as a gain medium and without the need for any adaptive optics in the resonator [37]. This latest achievement paves the way to passively modelocked oscillators in the kW average power regime.

B. Modelocking of High-Power TDLs

The TDL geometry is ideally suited for passive modelocking with high average power and high pulse energy. Compared to other bulk and fiber approaches, the use of a thin gain medium provides amplification with small interaction volume, which results in low accumulated nonlinearities. However, the resulting low-gain per disk pass typically leads to low gain per roundtrip in standard resonator geometries. Therefore, ultrafast TDLs operate with intracavity average powers and peak powers significantly higher than the corresponding output (see Table I), and modelocking instabilities need to be tackled. This represents one of the main challenges for pulse energy scaling of this technology. However, it is worth noting that the high intracavity peak powers available inside TDLs can also be exploited for certain applications in a similar way to passive enhancement cavities. This approach is particularly promising for HHG and XUV frequency combs [34].

The most common regime of operation of modelocked TDLs is the soliton modelocking regime [43]–[46], started and stabilized by a semiconductor saturable absorber mirror (SESAM) [47], [48]. The resulting sech^2 shaped transform-limited pulses even at extremely high output power levels are an inherent advantage of this type of oscillators compared to systems relying on recompression of chirped pulses such as chirped pulse

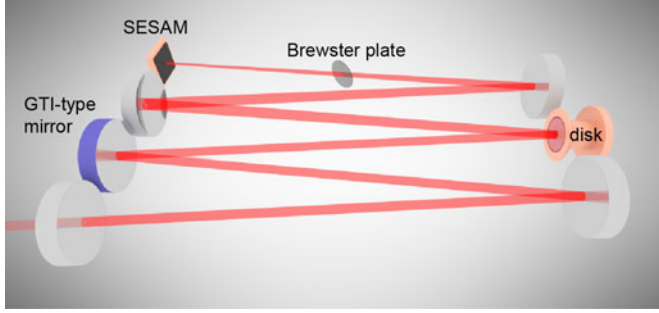


Fig. 5. Schematic layout of a SESAM-modelocked TDL.

amplification (CPA). SESAMs are perfectly suited for power and energy scaling of high-power oscillators, as they can be designed to have high-damage thresholds in order to withstand extreme intracavity conditions [49]. When designed appropriately, they benefit from the same power scaling features as the thin disk gain medium: the beam area on the SESAM and the pulse energy can be scaled by the same factor, keeping a constant level of saturation.

In Fig. 5 we present the layout of a typical SESAM soliton-modelocked TDL. The laser oscillator footprint is not significantly more complex than that of a standard low-power oscillator. In the most standard layout, the disk is used as a folding mirror in a linear cavity, but ring TDLs have also recently been demonstrated in the Kerr Lens Modelocked (KLM) regime [50]. For some specific applications, such as intracavity HHG, unidirectional oscillation is preferred, justifying the use of a ring oscillator. However, in this configuration, the gain per roundtrip is half that of a linear cavity. This increases the difficulties linked to high intracavity average and peak powers when the oscillator is operated efficiently. In addition, the layout for a few MHz high-energy ring cavity becomes easily impractical due to the length of the resonator (for example in a ring cavity, a 3 MHz modelocked oscillator has a length of ≈ 100 m). The difficulties linked to increasing the resonator length will be discussed in Section III. In this paper, we focus on output power and pulse energy of modelocked TDLs. In this goal the linear resonator is then preferable to the ring configuration, and we will focus the discussion on this type of resonator.

During each round-trip in the cavity, the circulating pulse accumulates a certain nonlinear phase due to self-phase modulation (SPM). If the total phase shift due to SPM is not too strong (typically than some hundred mrad per roundtrip), the resulting spectral phase can be compensated by negative second-order group delay dispersion (GDD), typically introduced with negative dispersion mirrors. Provided that the SESAM has the correct parameters to start and stabilize the modelocking mechanism, a sech^2 soliton pulse is formed. Once the soliton is started and stabilized, its full-width half maximum pulse duration τ_p only depends on the balance between dispersion and SPM, according to the well-known soliton formula [46]:

$$\tau_p = 1.76 \frac{2|D|}{\gamma E_p} \quad (1)$$

where D is the total GDD per roundtrip in s^2 , E_p the intracavity pulse energy, and γ the total cavity SPM coefficient expressed in rad/W and given for a Gaussian beam by:

$$\gamma = 2 \frac{kn_2 L_{SPM}}{\pi \omega_0^2} \quad (2)$$

where n_2 is the nonlinear refractive index of the SPM medium expressed in m^2/W , L_{SPM} the total length of the SPM medium as seen by the pulses in one roundtrip of the resonator, ω_0 the beam waist at the SPM medium and $k = 2\pi/\lambda$. Formula (2) is valid provided that the beam size does not change significantly throughout the length of the SPM medium, which is the case for example for the thin gain medium in TDLs or for a thin Brewster plate. For modelocked TDLs with very high pulse energies, the nonlinearity of the air inside the resonator is typically the main contribution to the SPM coefficient, and integration throughout the spot size distribution of a specific laser cavity is needed to evaluate the γ -factor. The corresponding formula will be presented and discussed in Paragraph II-E.

For modelocked TDLs that operate with a higher number of passes through the disk to increase the gain per roundtrip, the achievable pulse duration is longer and the soliton formula needs to be adapted to take into account the degree of output coupling [51]. As we aim to minimize complexity, we focus here on resonators with few passes through the disk, where the standard soliton formula can be applied. Although the final pulse duration achieved in this regime does not depend on the absorber parameters, the SESAM plays a crucial role in the stabilization of the pulses, as it can influence whether a targeted pulse duration can be reached in a stable configuration with a certain SPM and GDD balance in the resonator, and can affect the maximum tolerable SPM phase-shift per roundtrip.

Another important aspect for modelocking of high-power TDLs are Q-switching instabilities that can occur due to competing saturation effects of the gain and the absorber, in particular as large beam sizes are used on both components [52]. This has so far not represented a crucial limitation due to the very high intracavity pulse energies involved. However, as we move to kilowatt average powers, spot sizes on laser and absorber will be substantially increased and such instabilities could potentially become non negligible, in particular as this regime typically results in damage of intracavity components due to the very large peak powers reached.

An important property of these high-power modelocked oscillators is their intrinsically low noise level. This property is fairly uncritical for industrial applications, but is crucial for the targeted scientific applications, where noise of the driving source can be greatly amplified in the highly nonlinear processes involved.

The low gain per roundtrip inherent to the thin-disk geometry results in high quality factor (Q -factor) resonators in the standard cavity designs we focus on in this article. This allows for very low quantum noise limit, which can be aimed for with proper stabilization electronics. For many years, it was believed that the highly multimode pumping scheme of TDLs could degrade the noise properties of such high-power oscillators. In particular a complete stabilization (frequency and carrier-envelope phase)

was believed to be impossible. However, we recently demonstrated that the carrier envelope phase of this type of oscillator can be reliably detected and tightly stabilized to a reference [53], illustrating their outstanding noise properties. This opens an even larger range of applications for these sources in the field of frequency metrology and precision spectroscopy using these high-power sources as frequency combs. A detailed investigation of the noise properties of such high-power oscillators is currently in progress, which will allow to precisely compare their performance to amplifier systems delivering similar performance.

Other modelocking regimes have been explored in the thin-disk geometry. Recently, Kerr-lens modelocked TDLs have attracted attention as a modelocking regime where large fractions of the available gain bandwidth can be exploited [50], [54], [55]. In conventional KLM oscillators, the gain medium is the main source of nonlinearity and provides the necessary spatial Kerr lens for the modelocking mechanism. In a thin-disk oscillator, the gain medium is very thin and the laser beam radii on it are typically large, resulting in a negligible Kerr effect. Therefore, a separate Kerr medium is commonly used, for example a fused silica or undoped YAG plate placed at a focus in the resonator.

Although this type of modelocking mechanism applied to TDLs has gained significant ground in the past few years, they do not reach the peak power, average power, pulse energy and pulse duration performance demonstrated by SESAM soliton-modelocked TDLs so far, and it still remains unclear whether this type of oscillators can be energy scaled in a straightforward way.

In Kerr-lens modelocking, the sources of SPM and self-amplitude modulation (SAM) originate in one single cavity element. The resulting strong coupling of spatial and temporal effects can become detrimental at extremely high peak powers. Furthermore, this eliminates the possibility to optimize the strength of these two crucial parameters independently, which will pose increasing challenges as these oscillators approach several tens of kilowatts of intracavity average power and tens of millijoules of intracavity pulse energy. In contrast, in SESAM soliton modelocking, the SESAM parameters can be tuned for stable modelocking, and SPM can be adjusted independently for example by changing the air pressure inside the resonator, or simply by placing a Brewster plate in a loose focus in the resonator.

In addition, as the KLM mechanism relies on the spatial Kerr-effect, stable modelocking is closely related to the spatial resonator modes, which requires extremely careful cavity design, operation at the edge of resonator stability and intracavity elements with nearly zero thermal lensing. These design constraints will also be greatly increased when trying to operate with many tens of kilowatts of intracavity average power. In SESAM soliton modelocked TDLs, the cavity design can be optimized for robust single-fundamental mode at the center of the stability zone greatly simplifying cavity design constraints.

Therefore, we believe energy and power scaling by increasing the mode sizes in this type of oscillators will result in increased difficulties to operate such oscillators reliably. Taking into account these aspects, we believe that the next step in energy and

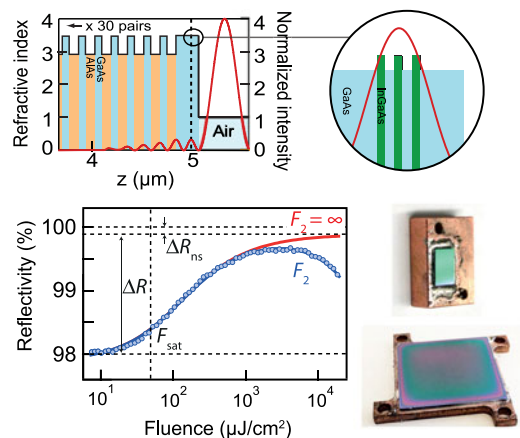


Fig. 6. Top: Structure and calculated standing wave intensity pattern for center wavelength normalized to incoming intensity [58] of a standard triresonant SESAM design and zoom into absorber section, in this case with three InGaAs QWs. Bottom left: Nonlinear reflectivity showing the typical saturation behavior of a SESAM. The macroscopic parameters are: F_{sat} : saturation fluence, ΔR : modulation depth, ΔR_{ns} : nonsaturable losses, F_2 : rollover coefficient. Bottom right: Picture of SESAMs used in high-power lasers. The large SESAM is 2.5 cm \times 2.5 cm and was designed for use in high-power TDLs.

average power scaling of modelocked TDLs will most likely still be achieved with SESAM soliton-modelocking.

The chirped-pulse oscillator (CPO) regime has also been explored in the thin-disk geometry [56], [57]. However, in the few demonstrated results, power scaling was hindered by the difficulty of achieving robust starting and operation of the oscillator. It is worth noting that this regime was possibly not explored further in this oscillator geometry because the limits of soliton modelocking have not been reached yet. This regime will most likely be explored in more detail as the intracavity peak powers inside modelocked oscillators are increased, reaching fundamental nonlinearity limits.

C. High-Power SESAMs

Modelocked TDLs operate at very high intracavity average power and pulse energy and therefore require SESAMs with adapted saturation and damage parameters.

SESAM structures are most commonly grown by Molecular Beam Epitaxy. A commonly used SESAM structure is illustrated in Fig. 6 (top). It consists of a distributed Bragg reflector for the laser wavelength (AlAs/GaAs) and an absorber section that is usually formed by one or several InGaAs quantum-wells (QWs) embedded in GaAs or AlAs and placed in an antinode of the resulting standing-wave electric field pattern.

The anti-resonant low-finesse SESAM is the most standard design used for high-power TDLs, because the resulting field in the semiconductor structure is low. An example of the characteristic reflectivity versus fluence response and different relevant macroscopic parameters are shown in Fig. 6.

The requirements for SESAMs in high-power TDLs are:

- 1) Large saturation fluence F_{sat} (typically $>100 \mu\text{J}/\text{cm}^2$) are preferred as they allow us to operate with moderate spot sizes. Spot size scaling relaxes these requirements,

but difficulties associated with beam distortions, thermal effects and laser resonator stability are then also increased. This will be discussed in more detail in Section III-A.

- 2) *Moderate to low modulation depths* ΔR in the order of one percent are typically sufficient given the small gain per roundtrip in TDLs. Modulation depths $>1\%$ up to a few percent are required in specific cases for example when the oscillator gain per roundtrip is increased by multiplying the number of gain passes through the disk, or when exploiting large fractions of the available gain bandwidth is targeted.
- 3) *Low nonsaturable losses* ΔR_{ns} are desired to avoid thermal effects.
- 4) *Rollover shifted to high fluences*: At very high fluences, effects such as two-photon absorption and/or free-carrier absorption result in a reduction of the reflectivity leading to a “rollover” in reflectivity, characterized by the fit parameter F_2 . Avoiding operation in this regime is crucial for TDLs, as it can favor multiple pulsing instabilities and damage [49], [59]–[61]. When the SESAM is operated beyond this “rollover”, several low-energy pulses circulating in the cavity can have a gain advantage compared to a single high-energy pulse [62].
- 5) *Damage*: In a recent investigation, this rollover was also identified to be the main cause of damage of the samples in the regime of operation of high-energy TDLs [49]. Therefore, shifting the rollover to higher fluences also results in samples with increased damage threshold.

Taking into account these requirements, guidelines were established to design SESAMs with such suitable parameters [49]. The most important findings are summarized here:

- 1) Damage is caused by energy deposited in the sample due to the rollover, which originates mainly from the layers of the structure with a strong two-photon absorption coefficient and a strong electric field. The use of antiresonant SESAMs and dielectric topcoatings is therefore beneficial for high damage threshold and a rollover shifted to high fluences.
- 2) The use of a dielectric top-mirror (for example a quarter-wave stack of $\text{SiO}_2 / \text{Si}_3\text{N}_4$) to increase the finesse of the structure increases the saturation fluence of the SESAM but reduces the modulation depth (the product of saturation fluence and modulation depth is constant for a given absorber section [49]), which is beneficial for the large pulse energies inside TDLs.
- 3) The damage threshold is nearly independent of the absorber section, therefore multiple QWs can be used to tune the modulation depth of the sample without changing its saturation fluence.
- 4) The growth temperature of the absorbers can be used to tune the nonsaturable losses [63]. A lower growth temperature results in a sample with a faster recovery time but higher nonsaturable losses. Soliton modelocking can tolerate absorber recovery times much longer than the pulse duration [43] and for high-energy modelocked TDLs the advantage of low nonsaturable losses is more crucial. Therefore, the absorber sections are typically

grown at $>300^\circ\text{C}$, resulting in typical nonsaturable losses $<0.1\%$.

It is important to notice that a shifted rollover allows us to tolerate much higher pulse fluences free of multiple pulsing instabilities. Therefore, increasing the saturation fluence to avoid oversaturation of the SESAM only makes sense for samples with an appropriately shifted rollover. In [18], stable mode-locking was achieved with a high saturation parameter of $S \approx 90$ which was only possible by using an optimized SESAM using our guidelines. Furthermore, the fluence where the rollover occurs scales with $\sqrt{\tau_p}$ [59], therefore lasers operating with longer pulse durations τ_p also tolerate higher fluences without multiple pulsing instabilities.

These guidelines indicate that a large number of QWs in combination with a high reflectivity dielectric top-mirror represents the best option for SESAMs for high-power oscillators. The SESAM used in our latest average power and pulse energy scaling results were fabricated using these guidelines and proved crucial to achieve this record performance.

Applying this concept further by increasing the number of QWs requires considering some fabrication constraints. A large number of QWs (typically >3) will make the fabrication more challenging as strain compensation will most likely be required to achieve samples with the required vanishing nonsaturable losses. Strain compensation is a common technique in semiconductor growth and can be considered for future samples.

Furthermore, a small number of QWs (typically up to 3) can be placed in the first antinode of the electric field, and a larger number can be placed in the consecutive antinodes. However, this requires adding significant amounts of semiconductor material where the electric field is strong, which can in turn decrease the damage threshold.

At the same time, a large number of dielectric top layers will ultimately increase the thickness of the structure and limit the thermal properties of the sample. The use of different dielectric materials with high refractive index contrast is an alternative to be considered that could partially solve this problem.

In the future targeted laser systems, larger spot sizes on the SESAMs will therefore most likely be required in combination with these high-damage threshold designs. We will discuss spot-size scaling of SESAMs in Section III-A.

D. Pulse Energy Scaling

For scaling the pulse energy (E_p) of modelocked TDLs both the average power P_{av} and the roundtrip time $T_r = 1/f_{rep}$ of the pulses can be increased according to

$$E_p = P_{av} T_r. \quad (3)$$

Typically, the available average power in fundamental single-transverse mode operation is limited given constraints imposed by the quality of the available disk and thermal aberrations of both the disk and other intracavity components. In order to maximize pulse energy, the roundtrip time of the pulses is increased thus reducing the repetition rate of the laser.

This can be achieved in a convenient way by inserting a Herriott-type multi-pass cavity (MPC) in the modelocked

TABLE I
OUTPUT AND INTRACAVITY PARAMETERS OF STATE-OF-THE-ART SESAM MODELOCKED TDLs

	Yb:YAG	Yb:YAG	Yb:YAG	Yb:YAG
output parameters				
average power	275 W	242 W	145 W	45 W
output pulse energy	17 μJ	80 μJ	41 μJ	11 μJ
repetition rate	16.3 MHz	3.0 MHz	3.5 MHz	4.0 MHz
pulse duration	583 fs	1070 fs	1120 fs	791 fs
peak power	25.5 MW	66.0 MW	32.2 MW	12.5 MW
intracavity parameters (OC rate)				
average power	(11%)	(25%)	(72%)	(11%)
pulse energy	2.38 kW	968 W	201 W	450 W
peak power	146 μJ	320 μJ	57 μJ	113 μJ
dispersion	220 MW	263 MW	45.2 MW	125.7 MW
gamma	-8100 fs ²	-28000 fs ²	-236000 fs ²	-20000 fs ²
gamma	0.34 mrad/MW	0.29 mrad/MW	37.5 mrad/MW	9 mrad/MW
nonlinearity				
main origin of remaining nonlinearity	remaining air pressure, nonlinearities in mirrors	remaining air pressure	air	helium, Brewster plate
total phase shift	75 mrad	76 mrad	1695 mrad	1125 mrad
technique to minimize total nonlinear phase shift	vacuum	vacuum	multiple gain passes	helium
SESAM				
F_{sat}	140 $\mu\text{J}/\text{cm}^2$	120 $\mu\text{J}/\text{cm}^2$	61 $\mu\text{J}/\text{cm}^2$	115 $\mu\text{J}/\text{cm}^2$
ΔR	0.95%	1.1%	3.5%	0.6%
ΔR_{ns}	< 0.1%	< 0.1%	not stated	< 0.1%
spot radius on SESAM	1.2 mm	1 mm	0.55 mm	0.7 mm
saturation parameter $S = F/F_{\text{sat}}$	25	90	100	60

resonator [64], (Fig. 7). This type of cell is most commonly used for absorption spectroscopy to increase the detection sensitivity by increasing the interaction length of light with a gas (also called long path absorption cells), but the concept can easily be adapted to be inserted in an ultrafast laser resonator [65], and has already proved successful in high-energy modelocked TDLs [18]. In [66], repetition rates below 1 MHz were obtained in a modelocked oscillator using this type of arrangement, but only at low power levels of ≈ 500 mW.

A q -preserving Herriott-type MPC operates in a similar way to $4f$ telescopes [67]: provided that the correct distance d between curved mirrors with a radius of curvature R is chosen, the q -parameter of the input Gaussian beam remains unchanged after propagation through the cell. They can then provide tens of meters of additional propagation L according to the formula:

$$L = nd = nR \left(1 - \cos \left(\frac{2\pi}{n} \right) \right), \quad (4)$$

where n is the number of passes on the curved surface with radius of curvature R . Such cells can be built in a compact layout and can be inserted at any position in the laser oscillator without modifying the beam parameters at the input.

Such an MPC was used in our latest pulse energy scaling result to 80 μJ , and this technique will most likely be used in future systems. We will discuss the design trade-offs in Section III.

E. Sources of Nonlinearity

In modelocked TDLs, the maximum tolerable nonlinear phase shift to achieve stable soliton modelocking is one of the most crucial elements that need to be taken into account. All sources of SPM need to be minimized in order to achieve the highest possible intracavity peak power. As illustrated in Fig. 5, the

thin-disk oscillator layout is ideally suited in this goal, as all intracavity elements are used in reflection.

The total nonlinearity of a modelocked resonator is characterized by estimating the SPM coefficient γ , taking into account all sources of nonlinearity seen by the pulses within one oscillator roundtrip. The main sources of SPM in a typical modelocked TDL are

- 1) Air (or corresponding gas) in the resonator

$$\gamma_{\text{atm}} = 4 \cdot \frac{2\pi}{\lambda} \int_{L_{\text{cav}}} \frac{n_{2,\text{gas}}}{S(z)} dz, \quad (5)$$

where $S(z)$ is the area of the Gaussian beam at a position z in the cavity, λ is the lasing wavelength in vacuum and $n_{2,\text{gas}}$ is the nonlinear refractive index of the considered gas at a given pressure.

- 2) Thin gain disk

$$\gamma_{\text{disk}} = 4 \cdot \frac{2\pi}{\lambda} \frac{n_{2,\text{disk}}}{S_{\text{disk}}} 2t_{\text{disk}}. \quad (6)$$

With the gain medium being very thin, it is typically assumed that the area of the beam does not vary along it, therefore we obtain (6) with t_{disk} the thickness of the disk and S_{disk} the corresponding laser beam area.

- 3) Brewster plate (BP)

$$\gamma_{\text{BP}} = 4 \cdot \frac{2\pi}{\lambda} \frac{n_{2,\text{BP}}}{S_{\text{BP}}} t_{\text{BP}}, \quad (7)$$

with t_{BP} the thickness of the BP and S_{BP} the corresponding area of the laser beam.

In low to medium energy TDLs, the main contribution to the total nonlinear phase shift originates from the Brewster plate introduced to control the amount of SPM and ensure a linearly

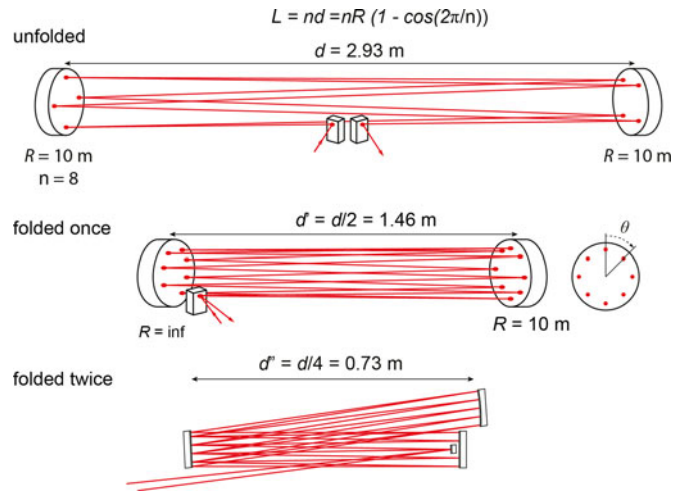


Fig. 7. Herriott-type multi-pass cavities can add several tens of meters of propagation in compact folded layouts. Here, we illustrate a multi-pass cell using a mirror with a radius of curvature $R = 10$ m and a number of passes $n = 8$.

polarized output. In the goal of minimizing the sources of non-linearity inside the oscillator, the Brewster plate can be replaced by a thin-film polarizer (TFP).

In high energy TDLs with very long resonator lengths the nonlinearity of the gas inside the cavity plays an increasingly important role in the total introduced SPM, and was identified as early as 2006 as one of the main limiting factors for energy scaling of such modelocked oscillators [67]. Several approaches have since then, been proposed to reduce this parasitic nonlinearity.

In Table I, we summarized these different methods, together with output parameters obtained from state-of-the-art high-energy modelocked TDLs. We present for each result the γ -parameter corresponding to each resonator design, the resulting phase shift per roundtrip at the intracavity peak power reached, and the necessary amount of dispersion used in the experiment to achieve soliton modelocking.

The first approach used to reduce the SPM coefficient was to flood the oscillator with Helium, which has a lower nonlinear refractive index n_2 than air at ambient pressure (see Table III). In this way, the first ultrafast oscillator with $>10 \mu\text{J}$ pulse energy [68] was achieved, and a clear confirmation that the previously limiting factor to achieve these high pulse energies was the parasitic contribution of the air to the nonlinearity [67].

Another interesting approach that proved successful for energy scaling of TDLs consists of reducing the ratio between intracavity power and output power of the oscillator [69]. This can be achieved by multiplying the number of gain passes through the disk and correspondingly increasing the output coupling rate. This is achieved at high laser efficiency as the gain per roundtrip is increased. This method was successfully implemented to demonstrate pulse energies $>40 \mu\text{J}$ at an average power of 145 W [70]. In this result, the laser resonator was operated at an output coupling rate of 72%, and 11 passes (44 single disk passes in a linear cavity with the disk used as a folding mirror) were used. The accumulated phase shift of >1 rad

per roundtrip (see Table I), and the observed Kelly sidebands in the spectral domain clearly indicate that further scaling was hindered by operation of the oscillator in air. This large amount of nonlinearity had to be compensated by an equally large amount of negative dispersion of $-237\,000 \text{ fs}^2$. Using this approach of multiplying the number of gain passes, both the complexity of the resonator and the requirements on the thermal lensing of the disk become extremely critical. With Yb:YAG, the requirements on the disk can be fulfilled using very thin disks contacted on diamond. For novel materials, where the disk and contacting quality is not yet as high, this point will be of more critical importance.

In order to reach the highest possible pulse energies in simple resonator geometries, a third approach was recently demonstrated which consists of operating the modelocked resonator in a pressure controlled environment by building the laser in a vacuum chamber [11]. This approach has an important number of advantages:

- 1) γ can be reduced by several orders of magnitude (see Table I), therefore tolerating orders of magnitude higher peak power.
- 2) Since there is very little SPM in such lasers, the dispersion required for soliton modelocking is moderate, even at very high intracavity pulse energies. This is beneficial as dispersive mirrors with large amounts of dispersion per bounce normally exhibit decreased thermal properties.
- 3) The nonlinearity can be controlled by varying the gas pressure in the chamber, therefore the pulse duration can be easily adjusted and optimized at a given pulse energy within the limit of the available GDD per roundtrip (see as an example Fig. 13).
- 4) Different gases can be used to flood the chamber for example in the goal of improving heat removal.
- 5) Pointing fluctuations and turbulences due to air fluctuations are avoided.
- 6) The oscillator operates in a clean environment, and no dust particles can degrade the intracavity components.

One point that needs to be considered however, are the increased thermal effects, in particular as we aim to keep simple geometries with low number of passes through the gain medium. For day-to-day long-term stability, low-absorption optics and water-cooling of different critical elements in the resonator becomes then a crucial requirement.

III. NEXT STEPS TOWARD MILLIJOULE LEVEL TDLs

So far, we have discussed general important aspects in the design of high-power modelocked TDLs, which have been crucial in achieving all the currently record-holding systems. However, moving toward the next generation will require further improvements. In the near future, we target modelocked oscillators with output pulse energies in the millijoule regime and average powers in the kilowatt range. In simple oscillator geometries with low gain per roundtrip, we therefore aim for intracavity powers of tens of kilowatts and pulse energies of tens of millijoules. This appears feasible given the latest scaling of CW fundamental transverse mode TDLs to 4 kW [37]. We will discuss in this

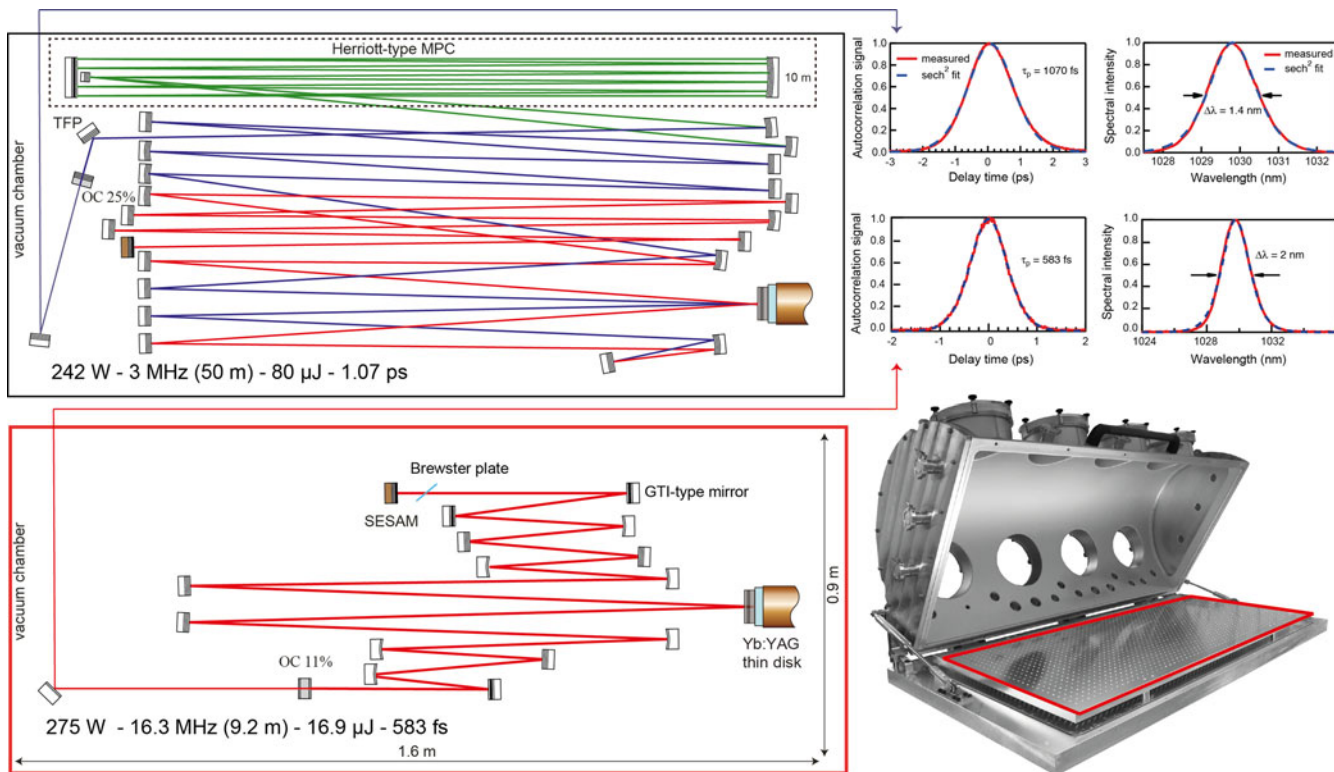


Fig. 8. Layout of the two oscillators used for power (275 W, bottom) and energy scaling (80 μ J, top) of modelocked TDLs, picture of the vacuum chamber and obtained experimental results in the two experiments (autocorrelation trace and optical spectrum of the sech^2 pulses). The large vacuum chamber was designed for maximum amount of flexibility. However, its footprint can be significantly reduced by optimizing for a given oscillator layout.

section what we believe will be the most important aspects to achieve these goals, based on the limitations currently observed in our two laser systems with the highest average power and the highest pulse energy. The results obtained, as well as the nonlinearity parameters, dispersion and SESAM parameters that we will refer to during this section are summarized in Table I. The layouts of the two oscillators, a picture of the vacuum chamber and the corresponding experimental results are presented in Fig. 8.

A. Milestone 1: Modelocking at the Kilowatt-Level

One of the most important limits for average power scaling of TDLs are thermal effects and damage that can occur in intracavity optics, in particular for oscillators operated at low pressure and with simple resonator geometries with a small number of gain passes through the disk. Already today, intracavity levels surpass the kW-level of average power (see Table I). In the latest result where we have demonstrated 275 W [11], reaching higher average powers was clearly hindered by thermal effects that occurred in the dispersive mirrors required for soliton modelocking. Such thermal effects manifest themselves as beam degradation that prevents us to reach higher power level. Therefore, significant improvement needs to be made in the thermal properties of these critical intracavity components as we aim for intracavity powers of several tens of kilowatts.

1) *Damage and Thermal Effects in Intracavity Optics:* The problem of thermal effects and damage of mirrors has been an important limitation in femtosecond passive enhancement cavities for many years [71]. These problems have partially been circumvented by using more adapted resonator designs with large-mode areas on the mirrors [72], which recently enabled impressive average power scaling to 400 kW intracavity power with 250 fs pulses at 250 MHz [73].

Although in a modelocked TDL the presence of gain allows us to tolerate higher amounts of losses compared to a high-finesse enhancement cavity, the limitations imposed by thermal effects and damage of cavity optics can be more severe for TDLs. In contrast to passive enhancement cavities, large amounts of negative GDD are required to achieve soliton modelocking at high pulse energy. In this goal, dielectric Gires-Tournois Interferometer (GTI)-type mirrors with significant field enhancement in the multilayer structure are commonly used. In this way, important amounts of GDD can be achieved per bounce, however typically with a reduced bandwidth [74]. The use of low-loss double chirped mirrors [75] can also be considered: however the low maximum achievable dispersion per bounce still remains impractical for the total overall amount of GDD required, therefore GTI-type mirrors still remain the preferred choice for such oscillators.

The large field enhancement in GTI-type mirror structures directly translates into a higher parasitic absorption compared to a standard highly reflective multi-layer stack, deteriorating

TABLE II
THERMAL CONDUCTIVITY AND COEFFICIENT OF THERMAL EXPANSION AT
ROOM TEMPERATURE OF DIFFERENT POSSIBLE SUBSTRATE
MATERIALS FOR DISPERSIVE MIRRORS.

Material	α $10^{-6} / ^\circ\text{C}$, at 25 $^\circ\text{C}$	κ W/(m·K)
Fused silica	0.5	1.4
Undoped YAG	8.2	14.0
Sapphire (avg)	5.8	24.1
Silicon Carbide	4	150
Diamond (CVD)	1	1800
Ultra Low Expansion (ULE) glass	$< 10^{-8}$	1.3
Zerodur	$< 10^{-6}$	1.5

The values were taken from datasheets of common providers of optical-grade substrates. However, it should be noted that values are given as a reference, but can vary for different manufacturers.

thermal properties and increasing losses. In high-power TDLs, pulses are at the moment still restricted to >500 fs. Therefore, the bandwidth requirements for flat GDD can easily be fulfilled by commercially available dispersive mirrors with high dispersion per bounce (typically < -500 fs² per bounce). However, the aforementioned thermal issues of GTI-type mirrors still represent a limitation in our latest average power and energy scaling results. Therefore, this represents one critical issue where significant improvement needs to be made.

Power absorbed in the coating results in heating of the mirror substrate leading to a deformation with a focal length f given by [76]:

$$f \propto \frac{\kappa}{\alpha} \frac{\omega_0^2}{P_{\text{abs}}}, \quad (8)$$

where P_{abs} is the absorbed power in the coating, which is proportional to the mirror absorption coefficient, κ the thermal conductivity (in W/m·K), α the coefficient of thermal expansion (in /K) and ω_0 the beam waist on the mirror.

According to Formula (8), the use of larger spots on these critical cavity components results in smaller thermal lensing. However, some resonator stability considerations need to be taken into account: the tolerable variation of a lens in a laser resonator is inversely proportional to the square of the spot size on this lens [41]. This has been discussed in the context of TDLs for the thermal lensing of the thin disk already in [40], where the increased difficulty of operating TDLs with large spot size areas in the gain disk is highlighted. The same arguments hold for other intracavity optics that exhibit thermal effects: in order to support resonators with larger spot sizes, mirrors with negligible thermal lensing are crucial.

Important efforts are therefore currently being made to design highly dispersive mirrors with very low absorption by using optimized material compositions, and using deposition techniques that support dense coatings [74]. However, commercially available solutions are not widespread, and very little data is reported on damage thresholds and thermal effects at MHz repetition rates and with sub-picosecond pulses. Nevertheless, as interest in such high-power oscillators increases, detailed investigations

are being carried out, which are slowly leading to significantly improved mirror structures [77].

Another potential improvement can be achieved by optimizing the properties of the mirror substrate. Improving the thermal conductivity alone is not sufficient: a good ratio between thermal expansion coefficient and thermal conductivity is required. Furthermore, the polishing quality and price of large substrates is another important aspect to be considered in the choice of a substrate. In Table II, different materials that could be used as mirror substrates are listed with their corresponding thermal conductivity and thermal expansion coefficient values. It appears that a good option consists of using materials with ultralow thermal expansion coefficient at room temperature such as Ultra Low Expansion glass (ULE, Corning) or Zerodur (Schott), which can be polished with similar quality to Fused Silica. Such improved low-absorption coatings in combination with optimized substrates should support the next average power-scaling step of modelocked TDLs.

2) *Flatness, Thermal Effects and Damage of SESAMs:* Thermal effects in SESAMs have so far, not represented a bottleneck for power scaling of modelocked TDLs. In modelocked operation, the power deposited as heat in the SESAM is very small, even at the high intracavity powers achieved so far. This is particularly the case as TDLs operate at very strong saturation of the absorber, therefore the deposited power into heat is in a good approximation restricted to the vanishing nonsaturable losses which are usually $< 0.1\%$.

However, as we target tens of kilowatts of intracavity power, this small fraction can become sufficient to create a thermal lens. The discussion of the previous paragraph concerning thermal lensing of dispersive mirrors then also applies to the SESAM: particularly as larger spot sizes will become more crucial to support tens of millijoules of intracavity pulse energy. Furthermore, the requirement on the flatness and contacting to the heatsink of the SESAM will become increasingly critical, even in cases where thermal lensing is negligible. As we can see in Table I, the spot radius used on SESAMs in high energy TDLs has so far never exceeded 1.2 mm. However, in our latest pulse energy scaling result to 80 μJ , the flatness of the SESAM already represented a limitation, as we could not significantly increase the spot size on the absorber without observing significant beam degradation and power loss. This is illustrated in Fig. 10, where the influence of varying the radius of curvature of the SESAM on the mode size distribution of the resonator used for our latest energy scaling result is shown for two different spot sizes on the SESAM (1 mm and 2 mm). The increased demands on the flatness and an eventual small thermal lensing of the SESAM for larger spot sizes is here clearly illustrated: already at a spot radius of 2 mm, a ROC smaller than 20 m results in significant changes of the laser spot size on the gain disk, which will degrade the beam quality. It is important also to notice that this only illustrates a spherical ROC, whereas in reality the surface quality is most likely more complex.

To fully benefit from the outstanding power scaling and excellent damage properties of SESAMs in the next generation of TDLs, these two aspects of better contacting and heat removal will therefore be crucial. In the standard SESAM geometry,

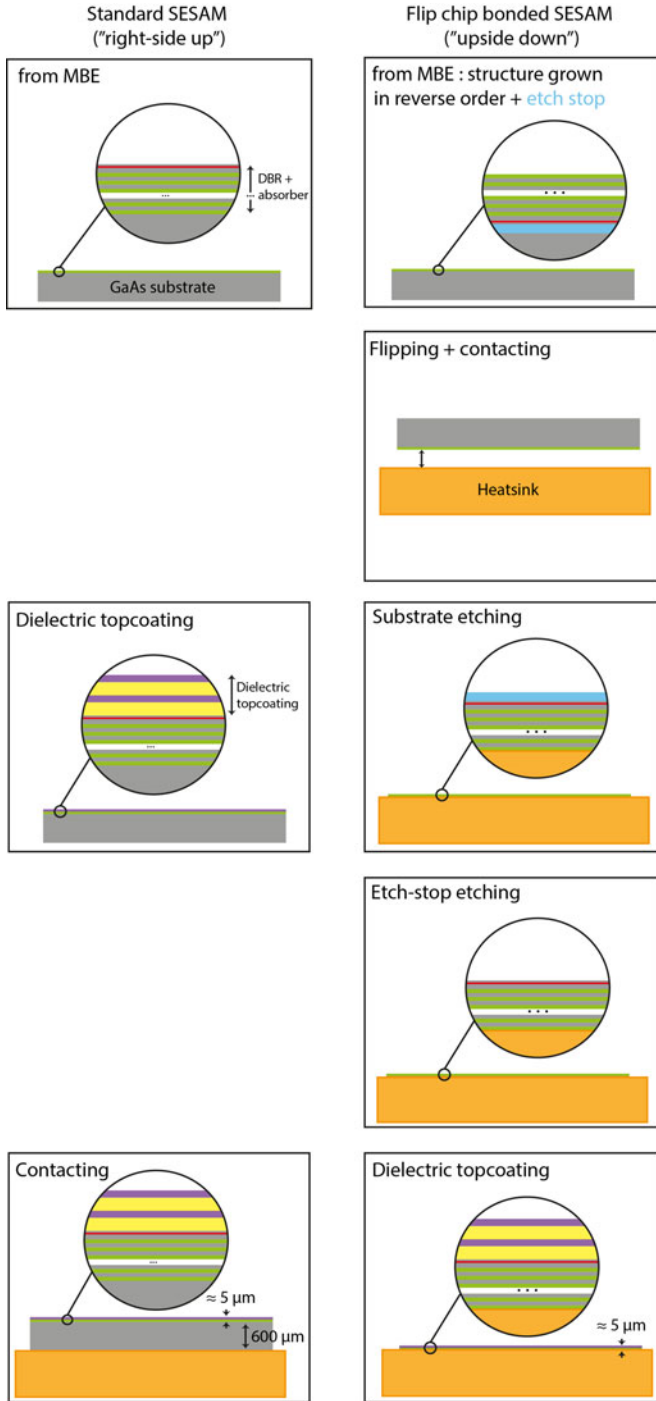


Fig. 9. Flip-chip bonding (“upside down”) SESAM fabrication procedure (right) versus standard (“right-side up”) SESAM.

a thick GaAs substrate (typically $\approx 600 \mu\text{m}$ thick) below the thin SESAM (typically $\approx 5 \mu\text{m}$ thick) limits thermal transport. A well-known technique to improve thermal management of semiconductor lasers is flip-chip bonding [78]. The same technique can be applied to SESAMs for high-power oscillators. It consists of growing the semiconductor structure in reverse order and then removing the substrate by selective etching (see Fig. 9). The resulting structure is then only a few μm thick and

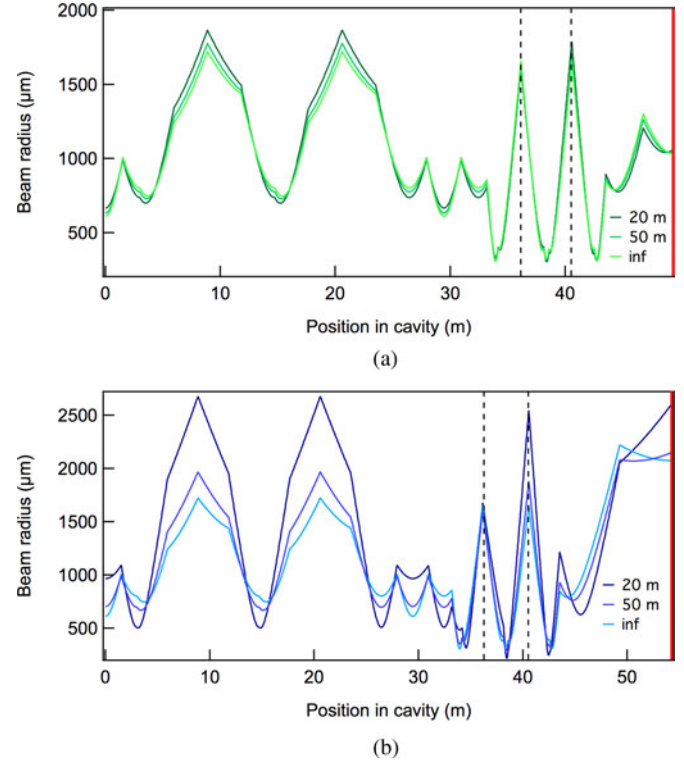


Fig. 10. Effect of an decrease of the ROC of the SESAM on the spot size distribution of the resonator used for our latest energy scaling result for a 1 mm (top) and b 2 mm (bottom) spot size radius on the SESAM. The increased spot size on the SESAM is achieved by modifying the magnification of the telescope in the resonator arm where the SESAM is placed, which results in no change of the mode size distribution in the rest of the cavity layout. The dashed line indicates the position of the disk, and the red line, the position of the SESAM.

can be cooled extremely efficiently if contacted on an appropriate heatsink (see for example Table II). Processing of such samples is however more challenging than the standard structures. In order to support the desired spot size scaling, large samples need to be fabricated. The surface quality needs to be excellent and homogeneous in large areas, which is challenging with chemical etching. Nevertheless, we successfully fabricated a large sample ($2.5 \times 2.5 \text{ cm}$), which is currently being tested for surface roughness, flatness and operation in a modelocked TDL with significantly larger spot sizes.

Using these large samples with improved flatness and thermal properties, we target upside down SESAMs with a uniform ROC larger than 100 m. In the laser layout of our $80 \mu\text{J}$ TDL, this should support spot radius $> 3 \text{ mm}$ which would already allow us to increase our intracavity pulse energy by nearly a factor of 10.

B. Milestone 2: Pulse Energy Scaling to the Millijoule Regime

1) *Increasing the Resonator Length Using Herriott-type MPCs:* In order to achieve the highest possible pulse energy at a given output power the most straightforward approach is to increase the roundtrip time of the pulses as described in II.D, by adding a Herriott-type MPC. In our latest energy scaling result to $80 \mu\text{J}$ [18], we used a MPC with $n = 8$ and $R = 10 \text{ m}$ which was folded once, with which we were able to increase our cavity

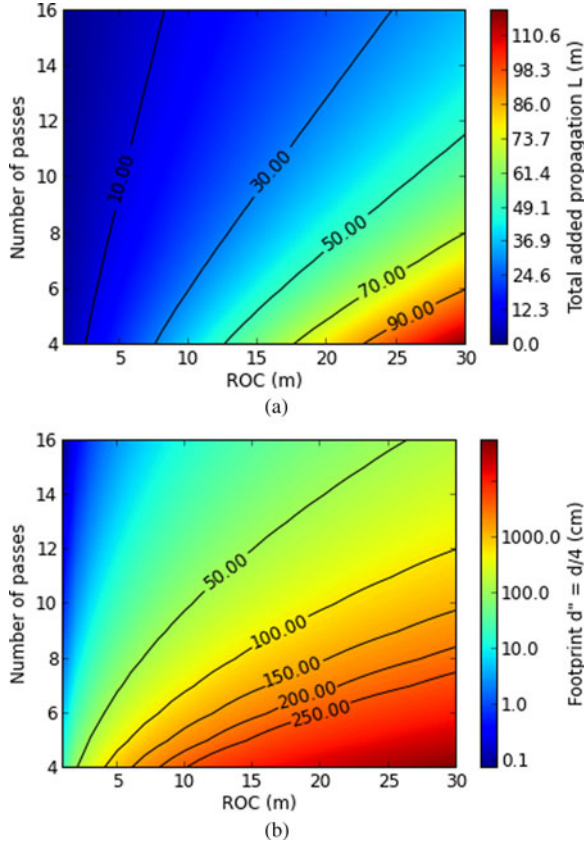


Fig. 11. (a) Total added distance (color map) as a function of radius of curvature and number of passes of a q -preserving Herriott type MPC. (b) Footprint of MPC (folded two times) as a function of radius of curvature and number of passes.

length by 23.4 m and achieve modelocking at a repetition rate of 3 MHz. Reducing the repetition rate even further would allow us to reach even higher pulse energies. However, for significantly longer cavities, design considerations such as the overall insertion loss and the footprint of the layout need to be considered. One should also not forget that high repetition rates are desired for the targeted applications; therefore reducing the repetition below 1 MHz is not of interest.

In the design of such MPCs we have two degrees of freedom: the radius of curvature R of the MPC mirror, and the number of passes n . In Fig. 11(a), we plotted the total added propagation distance (color map) D as a function of R and n using Formula (4), and in Fig. 11(b), the footprint of such an MPC when folded two times. Note that in these figures the color map is just indicative to illustrate the trend, as the number of bounces can just be discrete. In Fig. 12 we plot the total insertion loss versus the number of bounces on mirrors for a reflectivity range of the MPC mirrors between 99.8% and 99.98%. In this figure, the loss of an MPC folded two times with $n = 8$ is represented on the vertical axis by 32 bounces.

A compromise needs to be made between the desired added propagation distance, the footprint of the MPC and the insertion loss: as an example for a repetition rate of 2 MHz, the total linear resonator length is 75 m, a MPC with ≈ 70 m added propagation

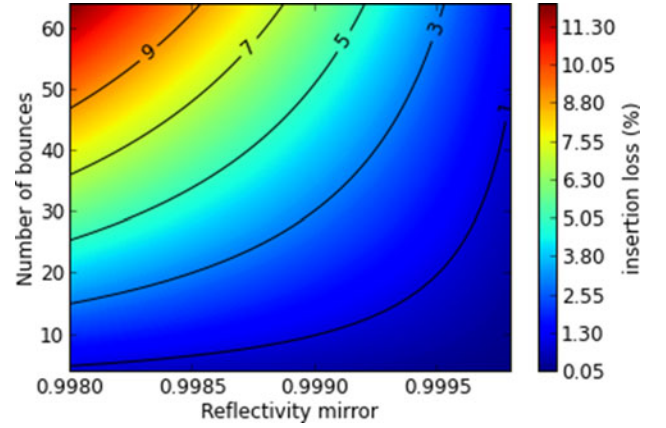


Fig. 12. Total loss in % of Herriott-type MPCs versus number of passes on the optics for different reflectivities of the MPC mirrors. The loss of an MPC folded times times with $n = 8$ corresponds to 32 bounces on mirrors.

distance is therefore desired. This can be achieved at a fixed number of bounces n by increasing the radius of curvature R , but this results in a significantly increased footprint.

Increasing the number of passes can then again reduce the footprint. However, this can only be achieved up to a certain extent given tolerable insertion losses and the need for very large optics. The requirements on the reflectivity of the used mirrors are then increased as well. In particular, the use of simple resonators with low gain per roundtrip, which will be sensitive to losses, makes these requirements more stringent.

Reducing the repetition rate of TDLs to < 2 MHz will therefore require the use mirrors with very high reflectivity ($> 99.95\%$), which will be supported by the development of low-absorption coatings discussed in Section III-A. The footprint of the oscillator will then also be increased: other novel MPC designs may then have to be considered in combination with techniques to reduce the overall insertion losses [79].

Therefore, we believe the next energy scaling step will not target repetition rates < 2 MHz. Further increase in pulse energy will most likely require an increase of the average output power.

2) *Nonlinearity*: We highlighted in II-E that one of the crucial difficulties for energy scaling of TDLs is to sufficiently reduce parasitic nonlinearities that, at very high pulse energies, can result in excessive phase shifts that destabilize soliton modelocking. The most promising approach for further scaling of modelocked TDLs is to operate the modelocked laser in a pressure-controlled environment, thus reducing the parasitic nonlinearity of the air in the resonator by several orders of magnitude. We believe that the next energy scaling step will most likely be achieved by using this method. This was the approach used in both our latest average power and energy scaling results. In both these results, the maximum pulse energy was reached at the lowest vacuum achievable with our scroll pump (≈ 0.5 mbar) raising the question of how to further increase the pulse energy.

The most straightforward first step to increase the pulse energy is to increase the amount of negative dispersion per roundtrip, which will allow us to tolerate larger nonlinear phase

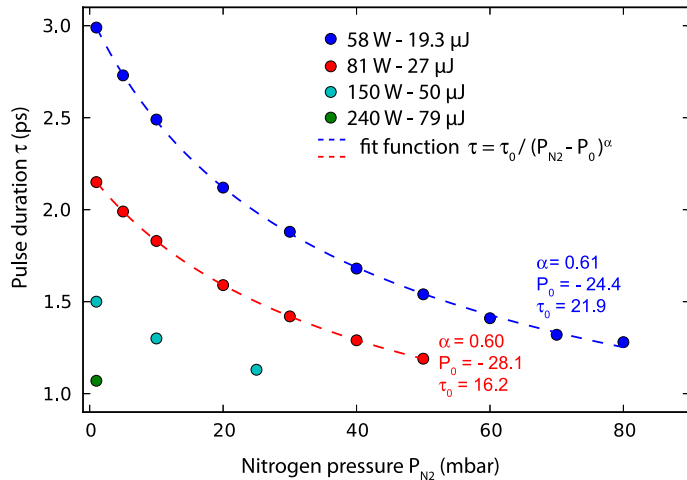


Fig. 13. Measurement of pressure dependent pulse duration. The different curves are obtained at a fixed pulse energy, by increasing the pressure of N_2 . All measurements were performed using the TDL that demonstrated 80 μJ of pulse energy. The data obtained for the highest pulse energies are not fitted because the amount of points is insufficient for a correct fit.

shifts. As indicated by the results obtained in [70], total phase shifts of >1 rad can be tolerated in modelocked operation with a total dispersion of 237 000 fs^2 . In our latest energy scaling result, the total nonlinear phase shift is less than ten times lower (see Table I). We therefore expect to be able to increase the intracavity pulse energy simply by a similar factor by increasing the amount of dispersion. However, to achieve this with simple resonator geometries, this will require the above-mentioned improvement in the thermal properties of such dispersive optics, which is at the moment one important bottleneck. In our current results, the dispersion in the cavity is typically minimized to avoid thermal effects and reach the highest possible average power.

Further energy scaling will require a more important reduction of the SPM coefficient. Reduction of the air pressure to even lower vacuum levels can be achieved by using for example a turbo pump. However, as the influence of the air in the resonator becomes smaller with lower gas pressure, other contributions, which were so far considered negligible, can become the dominant source of nonlinearity. Therefore, a further reduction of the pressure will not necessarily represent any significant advantage and the maximum reachable pulse energy will clamp. In this case, reducing the SPM factor by several orders of magnitude by reducing the gas pressure does not represent a significant advantage. Ideally one would want to operate the oscillator in a more comfortable regime where a minimum amount of gas pressure is present and the pulse duration can be controlled. It is therefore crucial to investigate in more detail these sources of extra nonlinearity for further pulse energy scaling. Possible sources for these extra parasitic nonlinearities are the disk, the SESAM, and other intracavity optics, in particular multilayer structures with strong field enhancements.

As a first step, we are studying experimentally the dependence of the nonlinearity present in the chamber to the gas pressure using our oscillator that delivers up to 80 μJ of pulse energy. This

TABLE III
THERMAL CONDUCTIVITY κ AND NONLINEAR REFRACTIVE INDEX n_2 OF DIFFERENT GASES AT 1 ATM AND 25 °C

Gas	n_2	κ
	$10^{-19} \text{ cm}^2/\text{W}$	$\text{mW}/(\text{cm}\cdot\text{K})$
N_2	2.3 \pm 0.3 [81]	0.3110 [82]
Air	2.9 \pm 0.4 [81]	0.3092 [81]
Ar	1.4 \pm 0.2 [81]	0.2048 [82]
Ne	0.08 [83]	0.5462 [82]
O_2	5.1 \pm 0.3 [81]	0.3074 [82]
He	0.04 [83]	1.704 [82]

is crucial for an accurate prediction of the laser parameters of our future systems and can shine light on the above-mentioned extra sources of nonlinearity at low pressures.

We measured the pulse duration of the soliton pulse as a function of the pressure in the chamber for different constant pulse energies ranging from 20 μJ (58 W) to 79 μJ (240 W). The results are presented in Fig. 13. For a given pulse energy, the pulse duration decreases with gas pressure. For the highest pulse energy (79 μJ), an increase in the chamber pressure above base pressure resulted in modelocking instabilities. In [80], the dependence of the nonlinear refractive index to pressure for different gases was measured to be linear for pressures >0.05 mbar. According to the soliton formula, the pulse duration should then vary following a $1/P$ law. However, we experimentally observe a discrepancy from the expected behavior: the duration reduces slower than expected with pressure following a $1/(P - P_0)^{0.6}$ law. Furthermore, an offset P_0 that increases with pulse energy is necessary for a correct fit of our experimental data, which is a clear indication that extra parasitic nonlinearities are present. We are currently investigating this in more detail, and we believe this study will enable us to clearly evaluate the limits for future energy scaling.

However, it is worth noting that the use of laser resonators with larger mode areas on the disk, on cavity optics and on the SESAM discussed in IIIA, which will in any case be crucial for energy scaling, will most likely also reduce these parasitic nonlinear effects. This could then justify going to lower vacuum levels.

The use of other gases for controlling the SPM in the laser resonator is another parameter that can be optimized for scaling the pulse energy of TDLs. The thermal effects discussed in the previous sections will become increasingly severe as we reach tens of kilowatts of average power. The use of gases with good thermal conductivity and lower nonlinear refractive index than air at low pressures is an interesting alternative to contribute to eliminating the thermal load on the optics. In Table III, we list a number of possible gases with their nonlinear refractive index and thermal conductivity. Most data concerning the nonlinearity of gases was measured at 800 nm, but it gives a good enough approximation at our laser wavelength of 1030 nm. Among these gases, Helium appears to be the best candidate: it has a nonlinear refractive index nearly two orders of magnitude lower than air at the same pressure and has a higher thermal conductivity,

relaxing the requirements on the pressure level and the thermal effects on intracavity optics.

Given this discussion, we believe that the next energy scaling step with TDLs will therefore operate in a pressure controlled He environment, and will benefit from an increase in the total amount of dispersion in the resonator.

C. Milestone 3: Pulse Duration Considerations

Until now, we have restricted our discussion to average power and pulse energy scaling. As we mentioned in the introduction, one important further aspect that will be crucial in future systems is reducing the pulse duration obtained with record-high average power and pulse energy. Although current TDLs reach pulse durations well below 100 fs, they are still restricted to $<1 \mu\text{J}$ and $<10 \text{ W}$ of average power. We will not discuss here in detail the specific requirements to reach shorter pulses from high-power TDLs. However, we will mention the most important difficulties to be addressed, as it is also considered a crucial next step.

The challenges discussed until here all apply for TDLs with shorter pulse durations, and the next steps discussed in the previous paragraphs will help to support this goal. However, in the case of short pulses additional difficulties need to be taken into account:

- 1) As nonlinearities scale with peak power, reaching high energies will become increasingly challenging. Reaching the millijoule pulse energy level with sub-100 fs pulses will, for example, require ten times lower nonlinearity than in current Yb:YAG based oscillators with $\approx 1 \text{ ps}$ pulse duration.
- 2) The most important parameter to reach shorter pulses is the available gain bandwidth. Although many Yb-doped gain materials are available that support very short pulse durations, their broadband nature usually comes at the expense of reduced thermo-mechanical properties, and do not yet reach the quality available from Yb:YAG. Furthermore, these materials are in many cases not commercially available. Significant progress in the quality of these materials and their contacting techniques will be an important aspect to extend the current record performance of TDLs to the short pulse regime.
- 3) The requirements on the SESAMs become more stringent as the pulse duration is decreased. In particular, the two-photon absorption coefficient of semiconductors scales proportionally to the pulse duration, and the rollover fluence in reflectivity with the square root of the pulse duration. Furthermore, even in the soliton modelocked regime, reaching very short pulse durations usually requires somewhat higher modulation depths and faster SESAMs, which typically result in higher nonsaturable losses and increased thermal effects. Therefore, applying our guidelines for high-damage threshold SESAMs specifically designed for short pulse generation will be essential to support this goal.

In the near future, we expect the quality of the available gain materials to significantly improve, supporting average power and pulse energy scaling in sub-100 fs pulse regime. Detailed understanding of the specific requirements of SESAMs for short

pulse durations from TDLs has already been done [25]. In combination with high-damage threshold designs [49] the extra difficulties should be overcome in a straightforward fashion. As a first step, we expect to reach the 100 W level with short pulse durations in the near future.

IV. GUIDELINES, CONCLUSION AND OUTLOOK

The performance of SESAM-modelocked high-power TDLs has recently reached new frontiers in average power (275 W) and pulse energy (80 μJ) available directly from an ultrafast oscillator. This recent progress seems to indicate that there are no major roadblocks that prevent the so-far exponential increase of the available pulse energy and average power from such sources toward the kilowatt and millijoule level.

By evaluating the current limitations in our existing systems, we have identified the crucial points that will need to be addressed for these future steps. The most important findings are summarized here:

- 1) *Thermal effects*: Thermal effects in intracavity mirrors will become increasingly important as output average powers reach the kilowatt range. In particular, soliton modelocked TDLs require significant amounts of negative dispersion for pulse formation, which is most conveniently introduced with multi-layer mirrors with field enhancements. These mirrors typically show thermal effects that need to be tackled. Significant improvement in the thermal properties of these optics can be achieved by using dense coatings and improved substrates.
- 2) *SESAM*: Pulse energy and average power scaling will require both adapted saturation parameters and spot size scaling. The guidelines established in [49] will be applied and possibly extended to SESAMs with even higher saturation fluences, rollover fluence and damage threshold. Spot size scaling will be enabled by improving the contacting method of current large size SESAMs to stressless techniques, to achieve better surface quality. Possible thermal effects on the SESAM might also become increasingly important as larger spot sizes are used. In a similar way to the improved thermal properties of dispersive optics, we plan to improve heat removal of our SESAMs by substrate removal and contacting to better heatsinks.
- 3) *Nonlinearities*: The next steps in power and energy scaling will most likely be achieved by operating the modelocked oscillator in a pressure-controlled environment.

An increase in pulse energy by a factor of 10 can be achieved by increasing the amount of negative dispersion in the laser oscillator thus tolerating phase shifts up to the maximum allowed by stable soliton modelocking (typically up to a few radians). This will only be possible with the above-mentioned dispersive mirrors with improved thermal properties.

Ultimately pulse energy scaling will require further reduction of the SPM coefficient: this can be achieved by reducing the gas pressure further, but only up to a certain limit. This ultimate limit is set by parasitic nonlinearities, which were so far considered negligible, such as the disk or nonlinearities due to the penetration depth of the field

into the dielectric mirrors and the SESAM. These nonlinearities can however be reduced by operating with larger spot sizes on these components.

The next step in energy scaling will therefore most likely combine higher dispersion values, larger laser spot areas on critical components and lower vacuum levels. Nevertheless, as some control is desired for the amount of nonlinearity, operation with low/medium pressure is preferred. The choice of the gas used then also plays an important role. We believe operating with Helium will be the best option as this gas offers a good ratio between thermal conductivity and low nonlinear refractive index.

We believe millijoule pulse energies will be feasible directly from passively modelocked thin-disk oscillators using soliton modelocking in the near future, as we show here that we are currently far away from maximum tolerable nonlinearity levels. This will be supported by an increased widespread interest in the well-suited disk technology for ultrafast applications.

In the future, as we approach the limits of soliton modelocking, other strategies for reducing nonlinear phase shifts, such as the CPO regime might be investigated in more detail. In addition, the resulting high-power oscillators with low-noise and excellent pulse quality are outstanding candidates for further seeding booster amplifiers, possibly using CPA techniques, and eventually for coherent combination.

REFERENCES

- [1] T. Südmeyer, S. V. Marchese, S. Hashimoto, C. R. E. Baer, G. Gingras, B. Witzel, and U. Keller, "Femtosecond laser oscillators for high-field science," *Nat. Photon.*, vol. 2, pp. 599–604, 2008.
- [2] G. Steinmeyer, D. H. Sutter, L. Gallmann, N. Matuschek, and U. Keller, "Frontiers in ultrashort pulse generation: Pushing the limits in linear and nonlinear optics," *Science*, vol. 286, pp. 1507–1512, 1999.
- [3] M. Ferray, A. L'Huillier, X. F. Li, L. A. Lompré, G. Mainfray, and C. Manus, "Multiple-harmonic conversion of 1064 nm radiation in rare gases," *J. Phys. B, At. Mol. Opt. Phys.*, vol. 21, pp. L31–L35, 1988.
- [4] S. R. Leone, C. W. McCurdy, J. Burgdoerfer, L. S. Cederbaum, Z. Chang, N. Dudovich, J. Feist, C. H. Greene, M. Ivanov, R. Kienberger, U. Keller, M. F. Kling, Z. H. Loh, T. Pfeifer, A. N. Pfeiffer, R. Santra, K. Schafer, A. Stolow, U. Thumm, and M. J. J. Vrakking, "What will it take to observe processes in 'real time'?" *Nat. Photon.*, vol. 8, pp. 162–166, Mar. 2014.
- [5] L. Shah, M. E. Fermann, J. W. Dawson, and C. P. J. Barty, "Micromachining with a 50 W, 50 μ J, sub-picosecond fiber laser system," *Opt. Exp.*, vol. 14, pp. 12546–12551, Dec. 11, 2006.
- [6] B. Jaeggi, B. Neuenschwander, M. Zimmermann, L. Penning, R. DeLoor, K. Weingarten, and A. Oehler, "High throughput and high precision laser micromachining with ps-pulses in synchronized mode with a fast polygon line scanner," *Proc. SPIE, Laser Applications in Microelectronic and Optoelectronic Manufacturing (LAMOM) XIX*, 89670Q, vol. 8967, 2014.
- [7] J. Lopez, R. Kling, R. Torres, A. Lidolff, M. Delaigue, S. Ricaud, C. Hönniger, and E. Mottay, "Comparison of picosecond and femtosecond laser ablation for surface engraving of metals and semiconductors," *Proc. SPIE, Laser Applications in Microelectronic and Optoelectronic Manufacturing (LAMOM) XVII*, 824300, vol. 8243, 2012.
- [8] T. Eidam, S. Hanf, E. Seise, T. V. Andersen, T. Gabler, C. Wirth, T. Schreiber, J. Limpert, and A. Tunnermann, "Femtosecond fiber CPA system emitting 830 W average output power," *Opt. Lett.*, vol. 35, pp. 94–96, Jan 15, 2010.
- [9] J.-P. Negel, A. Voss, M. A. Ahmed, D. Bauer, D. Sutter, A. Killi, and T. Graf, "1.1 kW average output power from a thin-disk multipass amplifier for ultrashort laser pulses," *Opt. Lett.*, vol. 38, pp. 5442–5445, Dec. 15, 2013.
- [10] P. Russbuedt, T. Mans, J. Weitenberg, H. D. Hoffmann, and R. Poprawe, "Compact diode-pumped 1.1 kW Yb:YAG Innoslab femtosecond amplifier," *Opt. Lett.*, vol. 34, pp. 4169–4171, 2010.
- [11] C. J. Saraceno, F. Emaury, O. H. Heckl, C. R. E. Baer, M. Hoffmann, C. Schriber, M. Golling, T. Suedmeyer, and U. Keller, "275 W average output power from a femtosecond thin disk oscillator operated in a vacuum environment," *Opt. Exp.*, vol. 20, pp. 23535–23541, 2012.
- [12] A. Giesen, H. Hügel, A. Voss, K. Wittig, U. Brauch, and H. Opower, "Scalable concept for diode-pumped high-power solid-state lasers," *Appl. Phys. B*, vol. 58, pp. 365–372, 1994.
- [13] A. Giesen and J. Speiser, "Fifteen years of work on thin-disk lasers: Results and scaling laws," *IEEE J. Sel. Top. Quantum Electron.*, vol. 13, no. 3, pp. 598–609, May/June 2007.
- [14] A. Klenke, S. Breilkopf, M. Kienel, T. Gottschall, T. Eidam, S. Hädrich, J. Rothhardt, J. Limpert, and A. Tunnermann, "530 W, 1.3 mJ, four-channelled coherently combined femtosecond fiber chirped-pulse amplification system," *Opt. Lett.*, vol. 38, pp. 2283–2285, Jul. 1, 2013.
- [15] M. Baumgartl, C. Lecaplain, A. Hideur, J. Limpert, and A. Tunnermann, "66 W average power from a microjoule-class sub-100 fs fiber oscillator," *Opt. Lett.*, vol. 37, pp. 1640–1642, May 15, 2012.
- [16] T. Eidam, S. Hädrich, F. Roser, E. Seise, T. Gottschall, J. Rothhardt, T. Schreiber, J. Limpert, and A. Tunnermann, "A 325-W-average-power fiber CPA system delivering sub-400 fs pulses," *IEEE J. Sel. Top. Quant.*, vol. 15, no. 1, pp. 187–190, Jan./Feb. 2009.
- [17] C. Teisset, M. Schultze, R. Bessing, M. Haefner, S. Prinz, D. Sutter, and T. Metzger, "300 W Picosecond thin-disk regenerative amplifier at 10 kHz repetition rate," presented at the Adv. Solid-State Lasers Congr. Postdeadline, Paris, France, 2013, Paper JTh5A.1.
- [18] C. J. Saraceno, F. Emaury, C. Schriber, M. Hoffmann, M. Golling, T. Südmeyer, and U. Keller, "Ultrafast thin-disk laser with 80 μ J pulse energy and 242 W of average power," *Opt. Lett.*, vol. 39, pp. 9–12, Jan. 1, 2013.
- [19] F. Röser, T. Eidam, J. Rothhardt, O. Schmidt, D. N. Schimpf, J. Limpert, and A. Tunnermann, "Millijoule pulse energy high repetition rate femtosecond fiber chirped-pulse amplification system," *Opt. Lett.*, vol. 32, pp. 3495–3497, 2007.
- [20] Y. Zaouter, J. Boulet, E. Mottay, and E. Cormier, "Transform-limited 100 μ J, 340 MW pulses from a nonlinear-fiber chirped-pulse amplifier using a mismatched grating stretcher-compressor," *Opt. Lett.*, vol. 33, pp. 1527–1529, Jul. 1, 2008.
- [21] J. Aus der Au, G. J. Spühler, T. Südmeyer, R. Paschotta, R. Hövel, M. Moser, S. Erhard, M. Karszewski, A. Giesen, and U. Keller, "16.2 W average power from a diode-pumped femtosecond Yb:YAG thin disk laser," *Opt. Lett.*, vol. 25, pp. 859–861, Jun. 1, 2000.
- [22] P. Lacovara, H. K. Choi, C. A. Wang, R. L. Aggarwal, and T. Y. Fan, "Room-temperature diode-pumped Yb:YAG laser," *Opt. Lett.*, vol. 16, pp. 1089–1091, Jul. 15, 1991.
- [23] S. Ricaud, A. Jaffres, K. Wentsch, A. Sukanuma, B. Viana, P. Loiseau, B. Weichelt, M. Abdou-Ahmed, A. Voss, T. Graf, D. Rytz, C. Hnninger, E. Mottay, P. Georges, and F. Druon, "Femtosecond Yb:CaGdAlO₄ thin-disk oscillator," *Opt. Lett.*, vol. 37, pp. 3984–3986, 2012.
- [24] K. S. Wentsch, L. Zheng, J. Xu, M. A. Ahmed, and T. Graf, "Passively mode-locked Yb³⁺:Sc₂SiO₅ thin-disk laser," *Opt. Lett.*, vol. 37, pp. 4750–4752, Nov. 15, 2012.
- [25] C. J. Saraceno, O. H. Heckl, C. R. E. Baer, M. Golling, T. Südmeyer, K. Beil, C. Kränkel, K. Petermann, G. Huber, and U. Keller, "SESAMs for high-power femtosecond modelocking: Power scaling of an Yb:LuScO₃ thin disk laser to 23 W and 235 fs," *Opt. Exp.*, vol. 19, pp. 20288–20300, 2011.
- [26] T. Südmeyer, C. Kränkel, C. R. E. Baer, O. H. Heckl, C. J. Saraceno, M. Golling, R. Peters, K. Petermann, G. Huber, and U. Keller, "High-power ultrafast thin disk laser oscillators and their potential for sub-100-femtosecond pulse generation," *Appl. Phys. B*, vol. 97, pp. 281–295, 2009.
- [27] K. Beil, C. J. Saraceno, C. Schriber, F. Emaury, O. H. Heckl, C. R. E. Baer, M. Golling, T. Südmeyer, U. Keller, C. Kränkel, and G. Huber, "Yb-doped mixed sesquioxides for ultrashort pulse generation in the thin disk laser setup," *Appl. Phys. B-Lasers Opt.*, vol. 113, pp. 13–18, 2013.
- [28] F. Emaury, C. J. Saraceno, B. Debord, C. Fourcade Dutin, Frédéric, Jérôme, Thomas, Südmeyer, Fethab Benabid, and Ursula Keller, "Pulse Compression of a High-Energy Thin-Disk Laser at 100 W of Average Power using an Ar-filled Kagome-Type HC-PCF," in Proc. Conf. Lasers Electro-Opt., San Jose, CA, USA, 2013, p. JTh4J.1.
- [29] F. Emaury, C. F. Dutin, C. J. Saraceno, M. Trant, O. H. Heckl, Y. Y. Wang, C. Schriber, F. Gerome, T. Südmeyer, F. Benabid, and U. Keller, "Beam delivery and pulse compression to sub-50 fs of a modelocked thin-disk laser in a gas-filled Kagome-type HC-PCF fiber," *Opt. Exp.*, vol. 21, pp. 4986–4994, Feb. 25, 2013.

- [30] C. J. Saraceno, C. Schriber, F. Emaury, O. H. Heckl, C. R. E. Baer, M. Hoffmann, K. Beil, C. Kränkel, M. Golling, T. Südmeyer, and U. Keller, "Cutting-edge high-power ultrafast thin disk oscillators," *Appl. Sci.*, vol. 3, pp. 355–395, 2013.
- [31] K. Petermann, G. Huber, L. Fornasiero, S. Kuch, E. Mix, V. Peters, and S. A. Basun, "Rare-earth-doped sesquioxides," *J. Lumin.*, vol. 87–89, pp. 973–975, 2000.
- [32] R. Peters, C. Kränkel, S. T. Fredrich-Thornton, K. Beil, O. H. Heckl, C. R. E. Baer, C. J. Saraceno, T. Südmeyer, U. Keller, K. Petermann, and G. Huber, "Thermal analysis and efficient high power continuous-wave and mode-locked thin disk laser operation of Yb-doped sesquioxides," *Appl. Phys. B.*, vol. 102, pp. 509–514, 2011.
- [33] C. R. E. Baer, C. Kränkel, C. J. Saraceno, O. H. Heckl, M. Golling, R. Peters, K. Petermann, T. Südmeyer, G. Huber, and U. Keller, "Femtosecond thin disk laser with 141 W of average power," *Opt. Lett.*, vol. 35, pp. 2302–2304, Jan. 6, 2010.
- [34] C. J. Saraceno, S. Pekarek, O. H. Heckl, C. R. E. Baer, C. Schriber, K. Beil, C. Kränkel, G. Huber, U. Keller, and T. Südmeyer, "Self-referenceable frequency comb from an ultrafast thin disk laser," *Opt. Exp.*, vol. 20, pp. 9650–9656, 2012.
- [35] C. J. Saraceno, O. H. Heckl, C. R. E. Baer, C. Schriber, M. Golling, K. Beil, C. Kränkel, T. Südmeyer, G. Huber, and U. Keller, "Sub-100 femtosecond pulses from a SESAM modelocked thin disk laser," *Appl. Phys. B.*, vol. 106, pp. 559–562, 2012.
- [36] A. Diebold, F. Emaury, C. J. Saraceno, C. Schriber, M. Golling, T. Südmeyer, and U. Keller, "62-fs pulses from a SESAM mode-locked Yb:CALGO thin disk laser," *Opt. Lett.*, vol. 38, pp. 3842–3845, 2013.
- [37] T. Gottwald, V. Kuhn, S. Schad, C. Stolzenburg, and A. Killi, "Recent developments in high power thin disk lasers at TRUMPF laser," *Proc. SPIE*, vol. 8898, pp. 1–7, 2014.
- [38] M. Huonker, C. Schmitz, and A. Voss, "Laser amplifying system," U.S. Patent 6 963 592, Nov. 8, 2005.
- [39] Y. H. Peng, Y. X. Lim, J. Cheng, Y. Guo, Y. Y. Cheah, and K. S. Lai, "Near fundamental mode 1.1 kW Yb:YAG thin-disk laser," *Opt. Lett.*, vol. 38, pp. 1709–1711, May 15, 2013.
- [40] C. R. E. Baer, O. H. Heckl, C. J. Saraceno, C. Schriber, C. Kränkel, T. Südmeyer, and U. Keller, "Frontiers in passively mode-locked high-power thin disk laser oscillators," *Opt. Exp.*, vol. 20, pp. 7054–7065, Mar. 26, 2012.
- [41] V. Magni, "Multielement stable resonators containing a variable lens," *J. Opt. Soc. Amer. A.*, vol. 4, pp. 1962–1969, 1987.
- [42] S. Piehler, B. Weichelt, A. Voss, M. A. Ahmed, and T. Graf, "Power scaling of fundamental-mode thin-disk lasers using intracavity deformable mirrors," *Opt. Lett.*, vol. 37, pp. 5033–5035, Dec. 15, 2012.
- [43] F. X. Kärtner and U. Keller, "Stabilization of soliton-like pulses with a slow saturable absorber," *Opt. Lett.*, vol. 20, pp. 16–18, 1995.
- [44] R. Paschotta and U. Keller, "Passive mode locking with slow saturable absorbers," *Appl. Phys. B.*, vol. 73, pp. 653–662, 2001.
- [45] U. Keller, "Ultrafast solid-state laser oscillators: A success story for the last 20 years with no end in sight," *Appl. Phys. B.*, vol. 100, pp. 15–28, 2010.
- [46] F. X. Kärtner, I. D. Jung, and U. Keller, "Soliton mode-locking with saturable absorbers," *IEEE J. Sel. Top. Quantum Electron.*, vol. 2, no. 3, pp. 540–556, Sep. 1996.
- [47] U. Keller, K. J. Weingarten, F. X. Kärtner, D. Kopf, B. Braun, I. D. Jung, R. Fluck, C. Hönninger, N. Matuschek, and J. Aus der Au, "Semiconductor saturable absorber mirrors (SESAMs) for femtosecond to nanosecond pulse generation in solid-state lasers," *IEEE J. Sel. Top. Quantum Electron.*, vol. 2, no. 3, pp. 435–453, Sep. 1996.
- [48] U. Keller, D. A. B. Miller, G. D. Boyd, T. H. Chiu, J. F. Ferguson, and M. T. Asom, "Solid-state low-loss intracavity saturable absorber for Nd:YLF lasers: An antiresonant semiconductor Fabry-Perot saturable absorber," *Opt. Lett.*, vol. 17, pp. 505–507, 1992.
- [49] C. J. Saraceno, C. Schriber, M. Mangold, M. Hoffmann, O. H. Heckl, C. R. E. Baer, M. Golling, T. Südmeyer, and U. Keller, "SESAMs for high-power oscillators: Design guidelines and damage thresholds," *IEEE J. Sel. Top. Quantum Electron.*, vol. 18, no. 1, pp. 29–41, Jan./Feb. 2012.
- [50] K. Natsuki, A. Amani Eilanlou, T. Imahoko, T. Sumiyoshi, Y. Nabekawa, M. Kuwata-Gonokami, and K. Midorikawa, "High-pulse energy Yb:YAG thin disk modelocked oscillator for intracavity high harmonic generation," presented at the Adv. Solid-State Lasers Congr., Paris, France, 2013, Paper AF3A.
- [51] J. Neuhaus, D. Bauer, J. Kleinbauer, A. Killi, D. H. Sutter, and T. Dekorsy, "Numerical analysis of a sub-picosecond thin-disk laser oscillator with active multipass geometry showing a variation of pulse duration within one round trip," *J. Opt. Soc. Amer. B-Opt. Phys.*, vol. 27, pp. 65–71, Jan. 2010.
- [52] C. Hönninger, R. Paschotta, F. Morier-Genoud, M. Moser, and U. Keller, "Q-switching stability limits of continuous-wave passive mode locking," *J. Opt. Soc. Amer. B.*, vol. 16, pp. 46–56, Jan. 1999.
- [53] A. Klenner, F. Emaury, C. Schriber, A. Diebold, C. J. Saraceno, S. Schilt, U. Keller, and T. Südmeyer, "Phase-stabilization of the carrier-envelope-offset frequency of a SESAM modelocked thin disk laser," *Opt. Exp.*, vol. 21, pp. 24770–24780, 2013.
- [54] O. Pronin, J. Brons, C. Grasse, V. Pervak, G. Boehm, M. C. Amann, V. L. Kalashnikov, A. Apolonski, and F. Krausz, "High-power 200 fs Kerr-lens mode-locked Yb:YAG thin-disk oscillator," *Opt. Lett.*, vol. 36, pp. 4746–4748, 2011.
- [55] J. Brons, O. Pronin, M. Seidel, V. Pervak, D. Bauer, D. Sutter, V. L. Kalashnikov, A. Apolonski, and F. Krausz, "120 W, 4 μ J from a purely Kerr-lens mode-locked Yb:YAG thin-disk oscillator," presented at the Adv. Solid-State Lasers, Paris, France, 2013.
- [56] G. Palmer, M. Schultze, M. Siegel, M. Emons, U. Bünting, and U. Morgner, "Passively mode-locked Yb:KLu(WO₄)₂ thin-disk oscillator operated in the positive and negative dispersion regime," *Opt. Lett.*, vol. 33, pp. 1608–1610, 2008.
- [57] O. Pronin, J. Brons, C. Grasse, V. Pervak, G. Boehm, M. C. Amann, A. Apolonski, V. L. Kalashnikov, and F. Krausz, "High-power Kerr-lens mode-locked Yb:YAG thin-disk oscillator in the positive dispersion regime," *Opt. Lett.*, vol. 37, pp. 3543–3545, Sep. 1, 2012.
- [58] G. J. Spühler, K. J. Weingarten, R. Grange, L. Krainer, M. Haiml, V. Liverini, M. Golling, S. Schon, and U. Keller, "Semiconductor saturable absorber mirror structures with low saturation fluence," *Appl. Phys. B.*, vol. 81, pp. 27–32, 2005.
- [59] R. Grange, M. Haiml, R. Paschotta, G. J. Spuhler, L. Krainer, M. Golling, O. Ostinelli, and U. Keller, "New regime of inverse saturable absorption for self-stabilizing passively mode-locked lasers," *Appl. Phys. B.*, vol. 80, pp. 151–158, 2005.
- [60] E. R. Thoen, E. M. Koontz, M. Joschko, P. Langlois, T. R. Schibli, F. X. Kärtner, E. P. Ippen, and L. A. Kolodziejski, "Two-photon absorption in semiconductor saturable absorber mirrors," *Appl. Phys. Lett.*, vol. 74, pp. 3927–3929, Jun. 28, 1999.
- [61] T. R. Schibli, E. R. Thoen, F. X. Kärtner, and E. P. Ippen, "Suppression of Q-switched mode locking and break-up into multiple pulses by inverse saturable absorption," *Appl. Phys. B.*, vol. 70, pp. S41–S49, 2000.
- [62] J. Aus der Au, D. Kopf, F. Morier-Genoud, M. Moser, and U. Keller, "60-fs pulses from a diode-pumped Nd:glass laser," *Opt. Lett.*, vol. 22, pp. 307–309, 1997.
- [63] M. Haiml, U. Siegner, F. Morier-Genoud, U. Keller, M. Luysberg, R. C. Lutz, P. Specht, and E. R. Weber, "Optical nonlinearity in low-temperature-grown GaAs: Microscopic limitations and optimization strategies," *Appl. Phys. Lett.*, vol. 74, pp. 3134–3136, May 24, 1999.
- [64] D. R. Herriott and H. J. Schulte, "Folded optical delay lines," *Appl. Opt.*, vol. 4, pp. 883–889, Aug. 1965.
- [65] A. Sennaroglu and J. G. Fujimoto, "Design criteria for herriott-type multipass cavities for ultrashort pulse lasers," *Opt. Exp.*, vol. 11, pp. 1106–1113, May 5, 2003.
- [66] D. N. Papadopoulos, S. Forget, M. Delaigue, F. Druon, F. Balembois, and P. Georges, "Passively mode-locked diode-pumped Nd : YVO₄ oscillator operating at an ultralow repetition rate," *Opt. Lett.*, vol. 28, pp. 1838–1840, Oct. 1, 2003.
- [67] S. V. Marchese, T. Südmeyer, M. Golling, R. Grange, and U. Keller, "Pulse energy scaling to 5 μ J from a femtosecond thin disk laser," *Opt. Lett.*, vol. 31, pp. 2728–2730, Aug. 25, 2006.
- [68] S. V. Marchese, C. R. E. Baer, A. G. Engqvist, S. Hashimoto, D. J. H. C. Maas, M. Golling, T. Südmeyer, and U. Keller, "Femtosecond thin disk laser oscillator with pulse energy beyond the 10-microjoule level," *Opt. Exp.*, vol. 16, pp. 6397–6407, 2008.
- [69] J. Neuhaus, D. Bauer, J. Zhang, A. Killi, J. Kleinbauer, M. Kumkar, S. Weiler, M. Guina, D. H. Sutter, and T. Dekorsy, "Subpicosecond thin-disk laser oscillator with pulse energies of up to 25.9 microjoules by use of an active multipass geometry," *Opt. Exp.*, vol. 16, pp. 20530–20539, 2008.
- [70] D. Bauer, I. Zawischa, D. H. Sutter, A. Killi, and T. Dekorsy, "Mode-locked Yb:YAG thin-disk oscillator with 41 μ J pulse energy at 145 W average infrared power and high power frequency conversion," *Opt. Exp.*, vol. 20, pp. 9698–9704, 2012.
- [71] I. Pupezta, T. Eidam, J. Rauschenberger, B. Bernhardt, A. Ozawa, E. Fill, A. Apolonski, T. Udem, J. Limpert, Z. A. Alahmed, A. M. Azzeeer, A. Tunnermann, T. W. Hansch, and F. Krausz, "Power scaling of a high-repetition-rate enhancement cavity," *Opt. Lett.*, vol. 35, pp. 2052–2054, Jun. 2010.

- [72] H. Carstens, S. Holzberger, J. Kaster, J. Weitenberg, V. Pervak, A. Apolonski, E. Fill, F. Krausz, and I. Pupez, "Large-mode enhancement cavities," *Opt. Exp.*, vol. 21, pp. 11606–11617, May 6, 2013.
- [73] H. Carstens, N. Lilienfein, S. Holzberger, C. Jocher, T. Eidam, J. Limpert, A. Tunnermann, J. Weitenberg, D. C. Yost, A. Alghamdi, Z. Alahmed, A. Azzeer, A. Apolonski, E. Fill, F. Krausz, and I. Pupez, "Megawatt-scale average-power ultrashort pulses in an enhancement cavity," *Opt. Lett.*, vol. 39, pp. 2595–2598, May 1, 2014.
- [74] V. Pervak, O. Pronin, O. Razskazovskaya, J. Brons, I. B. Angelov, M. K. Trubetskov, A. V. Tikhonravov, and F. Krausz, "High-dispersive mirrors for high power applications," *Opt. Exp.*, vol. 20, pp. 4503–4508, Feb. 13, 2012.
- [75] N. Matuschek, F. X. Kärtner, and U. Keller, "Analytical design of double-chirped mirrors with custom-tailored dispersion characteristics," *IEEE J. Quantum Electron.*, vol. 35, no. 2, pp. 129–137, Feb. 1999.
- [76] W. Winkler, K. Danzmann, A. Rudiger, and R. Schilling, "Heating by optical-absorption and the performance of interferometric gravitational-wave detectors," *Phys. Rev. A*, vol. 44, pp. 7022–7036, Dec. 1, 1991.
- [77] I. B. Angelov, M. von Pechmann, M. K. Trubetskov, F. Krausz, and V. Pervak, "Optical breakdown of multilayer thin-films induced by ultrashort pulses at MHz repetition rates," *Opt. Exp.*, vol. 21, pp. 31453–31461, Dec. 16, 2013.
- [78] U. Keller, "Recent developments in compact ultrafast lasers," *Nature*, vol. 424, pp. 831–838, Aug. 14, 2003.
- [79] S. So and D. Thomazy, "Novel spherical mirror multipass cells with improved spot pattern density for gas sensing," in *Proc. Conf. Lasers Electro-Opt., CW3B.6*, 2012.
- [80] A. Börzsönyi, Z. Heiner, A. P. Kovacs, M. P. Kalashnikov, and K. Osvay, "Measurement of pressure dependent nonlinear refractive index of inert gases," *Opt. Exp.*, vol. 18, pp. 25847–25854, 2010.
- [81] E. T. J. Nibbering, G. Grillon, M. A. Franco, B. S. Prade, and A. Mysyrowicz, "Determination of the inertial contribution to the nonlinear refractive index of air, N₂, and O₂ by use of unfocused high-intensity femtosecond laser pulses," *J. Opt. Soc. Amer. B*, vol. 14, pp. 650–660, Mar. 1997.
- [82] S. Saxena, "Transport properties of gases and gaseous mixtures at high temperatures," *High Temp. Sci.*, vol. 3, pp. 168–188, 1971.
- [83] C. Bree, A. Demircan, and G. Steinmeyer, "Method for computing the nonlinear refractive index via Keldysh theory," *IEEE J. Quantum Electron.*, vol. 46, no. 4, pp. 433–437, Apr. 2010.



Clara J. Saraceno was born in Buenos Aires, Argentina, on September 13, 1983. She received the Dipl.Ing. and M.S. degrees from the Institut d'Optique Graduate School, Palaiseau, France, in September 2007, and the Ph.D. degree in Prof. Ursula Keller's group (Ultrafast Laser Physics) at Eidgenössische Technische Hochschule (ETH), Zurich, Switzerland, in 2012. From September 2007 to September 2008, she also received training in the R&D Department of the Ultrafast Division (RLS), Coherent, Inc., Santa Clara, CA, USA, where she

developed interest for ultrafast laser physics. Since 2013, she has been a Post-doctoral Fellow in collaboration between the Time and Frequency Laboratory at the University of Neuchâtel, Neuchâtel, Switzerland, and the Ultrafast Laser Physics group at ETH Zürich. Her current research interests include high-power ultrafast laser systems and their scientific and industrial applications.



Florian Emaury was born in Thouars, France, on September 18, 1987. He received the Dipl.Ing. and M.S. degrees from the Institut d'Optique Graduate School, Palaiseau, France, in September 2010. After a six-month training in the ultrafast fiber laser company, Fianium, Southampton, U.K., and a six-month training in the R&D Department of the Ultrafast Division (RLS) of Coherent, Inc., Santa Clara, CA, USA, he is currently working toward the Ph.D. degree in Prof. Ursula Keller's group (Ultrafast Laser Physics) at Eidgenössische Technische Hochschule

(ETH), Zurich, Switzerland. His current research interests include exploring the limits of high-power SESAM mode-locked thin disk oscillators and their applications to the field of high-harmonic generation at high repetition rate.



Cinia Schriber was born in Mexico City, on April 28, 1985. She received the M.S. degree in physics from the Eidgenössische Technische Hochschule (ETH), Zurich, Switzerland, in 2011. She is currently working toward the Ph.D. degree in Prof. Ursula Keller's Group (Ultrafast Laser Physics) at ETH Zurich.

Her current research interests include high-power ultrafast thin-disk lasers, with focus on the generation of short pulses, and their application in oscillator-driven high field physics experiments.



Andreas Diebold was born in Eutin, Germany, on January 17, 1989. In 2013, he received the M.S. degree in physics at Eidgenössische Technische Hochschule (ETH), Zurich, Switzerland, after studying at the National University of Singapore, Singapore. He is currently working toward the Ph.D. degree in Prof Ursula Keller's group (Ultrafast Laser Physics) at ETH.

His current research interests include mode-locked high-power thin-disk lasers including power scaling, ultrashort pulse generation and carrier-envelope phase stabilization, and laser-driven high-field physics experiments.



Martin Hoffmann was born in Dessau, Germany, on October 15, 1979. He received the M.S. degree in physics at Eidgenössische Technische Hochschule (ETH), Zurich, Switzerland, where he also received the Ph.D. degree in Prof. Ursula Keller's group (Ultrafast Laser Physics) for his research on optically and electrically pumped ultrafast semiconductor lasers. After that, he developed high-power semiconductor saturable absorber mirrors for Cyber Laser Inc., Tokyo, Japan.

He is currently with the University of Neuchatel, Neuchatel, Switzerland. His current research interests include new carrier envelope stabilization techniques for solid-state lasers, state-of-the-art dielectric coatings deposited with ion beam sputtering, with special focus on high-power ultrafast thin-disk lasers.



Matthias Golling was born in Sulz, Germany, on May 20, 1971. He received the Diploma degree in electrical engineering and the Ph.D. degree in engineering both from the University of Ulm, Ulm, Germany, in 1997 and 2004, respectively. He is currently the Leader of the molecular beam epitaxy activities at the Ultrafast Laser Physics Group, Eidgenössische Technische Hochschule (ETH), Zurich, Switzerland. His current research interests include the design and epitaxy of lasers and saturable absorbers.



Thomas Südmeyer studied physics at Leibniz University, Hanover, Germany, and ENS, Paris, France. He received the Ph.D. degree from Eidgenössische Technische Hochschule (ETH), Zurich, Switzerland, for research on the first mode-locked thin-disk lasers and novel nonlinear systems, in 2003. He is the Director of the Physics Department, University of Neuchâtel, Neuchâtel, Switzerland. In 1999, he started working on ultrafast lasers during an EU fellowship at Strathclyde University (Glasgow). During 2003 to 2005, he developed industrial laser solutions

at Sony Corporation, Tokyo. From 2005 to 2011, he investigated new concepts for ultrafast science and technology at ETH (Zurich), where he received the Habilitation degree. In 2011, he was appointed as the Full Professor and Head of the Time-Frequency Laboratory, University of Neuchâtel. He has been the Coordinator of several Swiss and European projects and was awarded with an ERC Starting Grant in 2011. He serves the research community as an Associate Editor for *Optics Express*. He is the author of more than 70 papers in international peer-reviewed journals, two book chapters, and he holds or applied for ten patents. His research interests are exploring and pushing the frontiers in photonics, metrology, and ultrafast science.



Ursula Keller (F'14) received the Physics "Diplom" from Eidgenössische Technische Hochschule (ETH), Zurich, Switzerland, in 1984, and the Ph.D. degree in applied physics from Stanford University, Stanford, CA, USA, in 1989. She was a Member of Technical Staff at AT&T Bell Laboratories, Murray Hill, NJ, USA, from 1989 to 1993. She joined ETH Zurich as a Professor of physics in 1993 and serves as a Director of the NCCR MUST which is an interdisciplinary research program launched by the Swiss National Science Foundation in 2010. She has published more

than 360 peer-reviewed journal papers and many book chapters and patents. She was a "Visiting Miller Professor" at the University of California, Berkeley, CA, in 2006, and a Visiting Professor at the Lund Institute of Technologies, Sweden, in 2001. Her current research interests involve exploring and pushing the frontiers in ultrafast science and technology. She received the EPS Senior Prize in 2011, the OSA Fraunhofer/Burley Prize in 2008, the Philip Morris Research Award in 2005, the first-place award of the Berthold Leibinger Innovation Prize in 2004, and the Carl Zeiss Research Award in 1998. She is a Fellow of OSA, EPS, and SPIE. She has been a Cofounder and a board member for Time-Bandwidth Products acquired by JDSU in 2014 and GigaTera from 2000 to 2003, a venture capital funded telecom company during the "bubble phase" which was acquired by Time-Bandwidth in 2003.